Probing the cosmic dipole in galaxy surveys

ASKAP and beyond

Oliver Oayda

PhD Candidate
Sydney Institute for Astronomy
The University of Sydney

Supervised by
Geraint Lewis
Tara Murphy

November 21, 2024

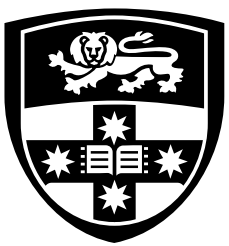

THE UNIVERSITY OF SYDNEY

EMU Cosmology Telecon

November 2024

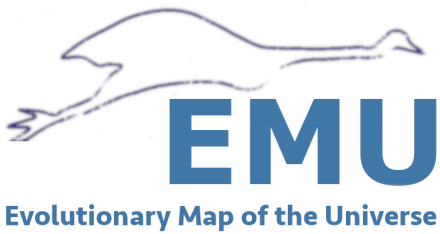

Agenda

Key Finding

- Dipole in RACS-low & NVSS is 2 to 3 times larger than expected.
- Is the CP in trouble, or are there systematics?

Background

The Cosmological Principle

On very large scales, the Universe is homogeneous and isotropic.

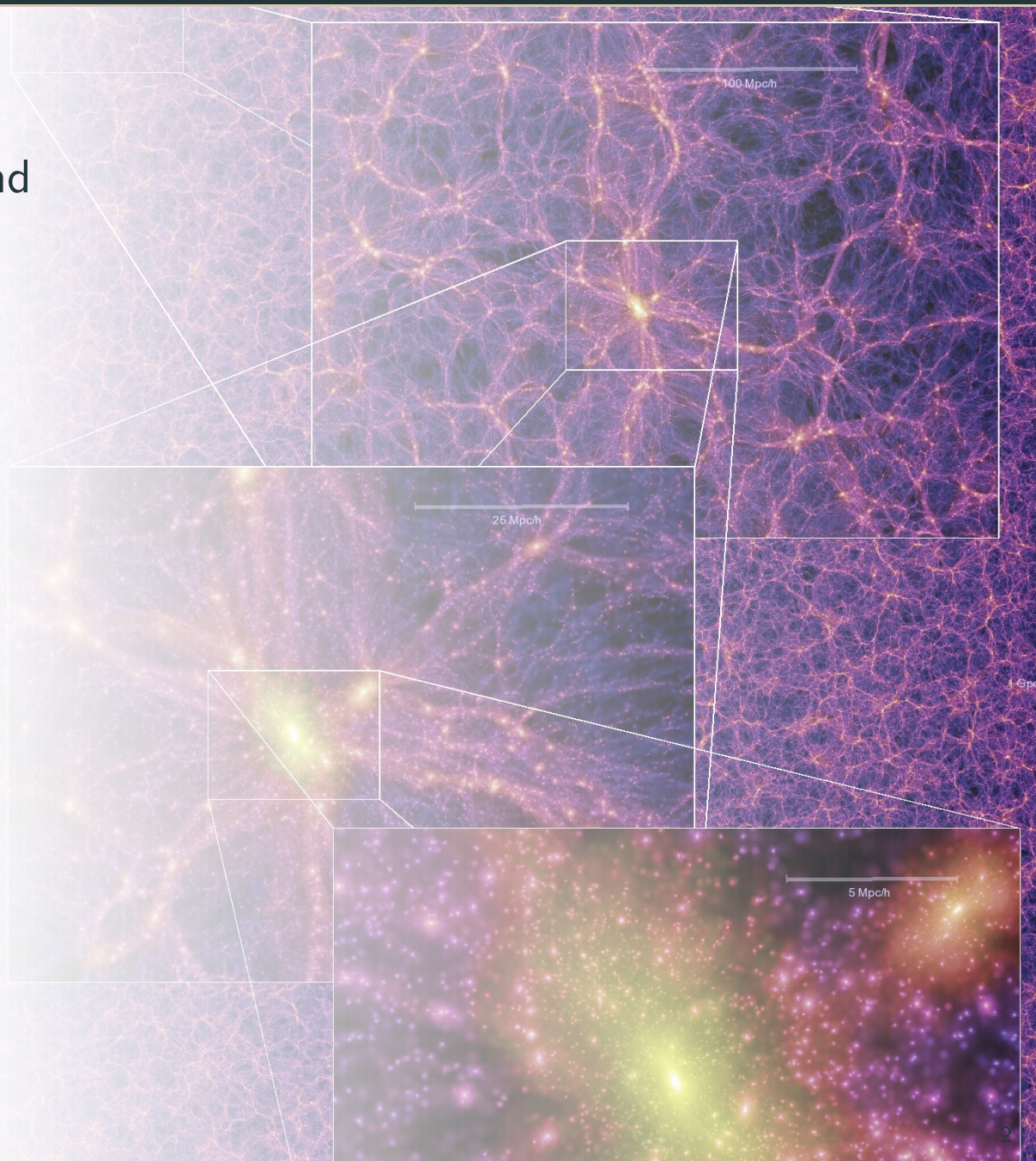

The Cosmological Principle

On very large scales, the Universe is homogeneous and isotropic.

Foundational assumption in current cosmological framework, e.g. FLRW, Friedmann world models, etc.

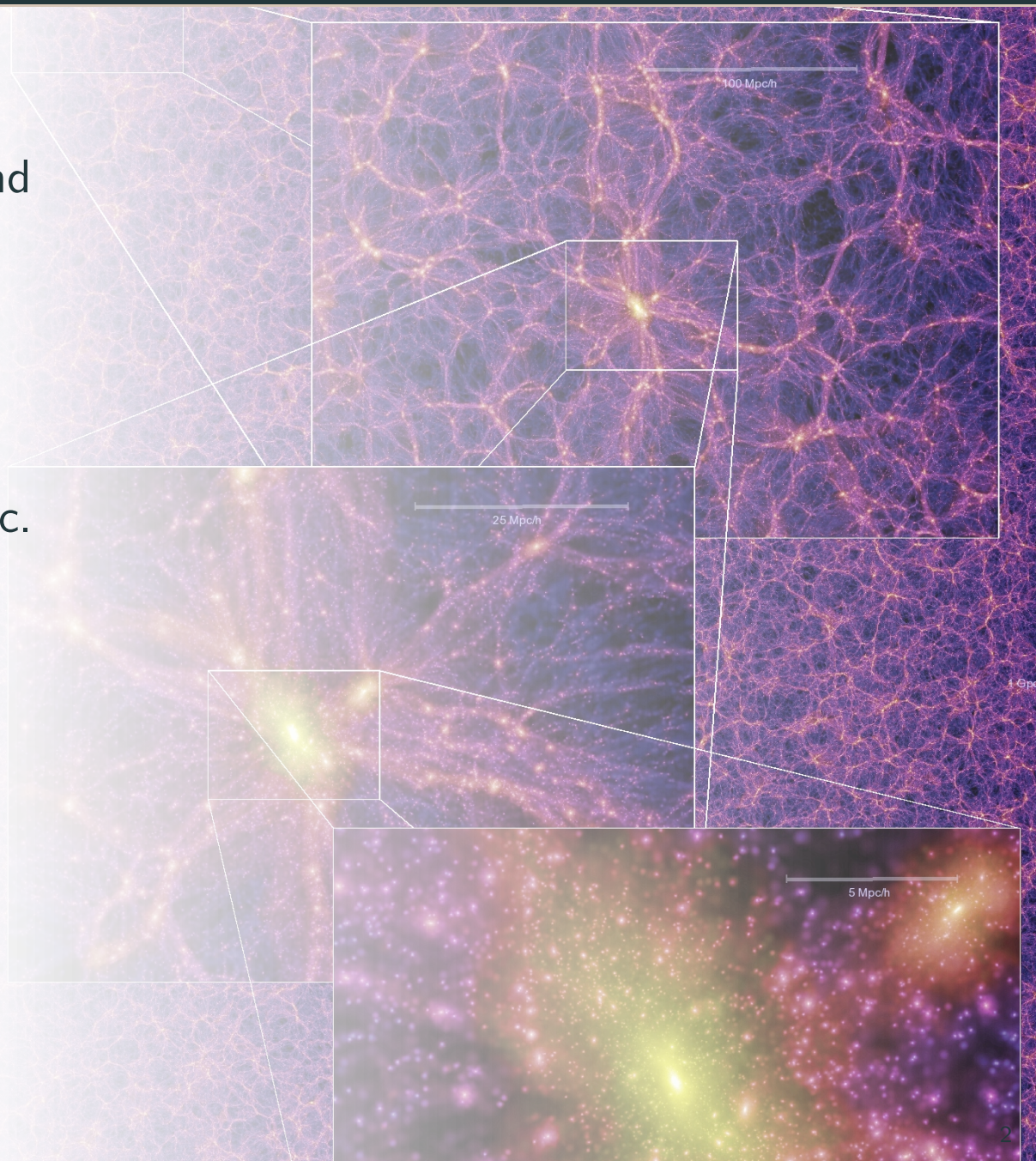

The Cosmological Principle

On very large scales, the Universe is homogeneous and isotropic.

Foundational assumption in current cosmological framework, e.g. FLRW, Friedmann world models, etc.

$$ds^2 = -c^2 dt^2 + a^2(t)\, d\Sigma^2$$

where

$$d\Sigma^2 = \frac{dr^2}{1 - \kappa r^2} + r^2 d\Omega^2$$

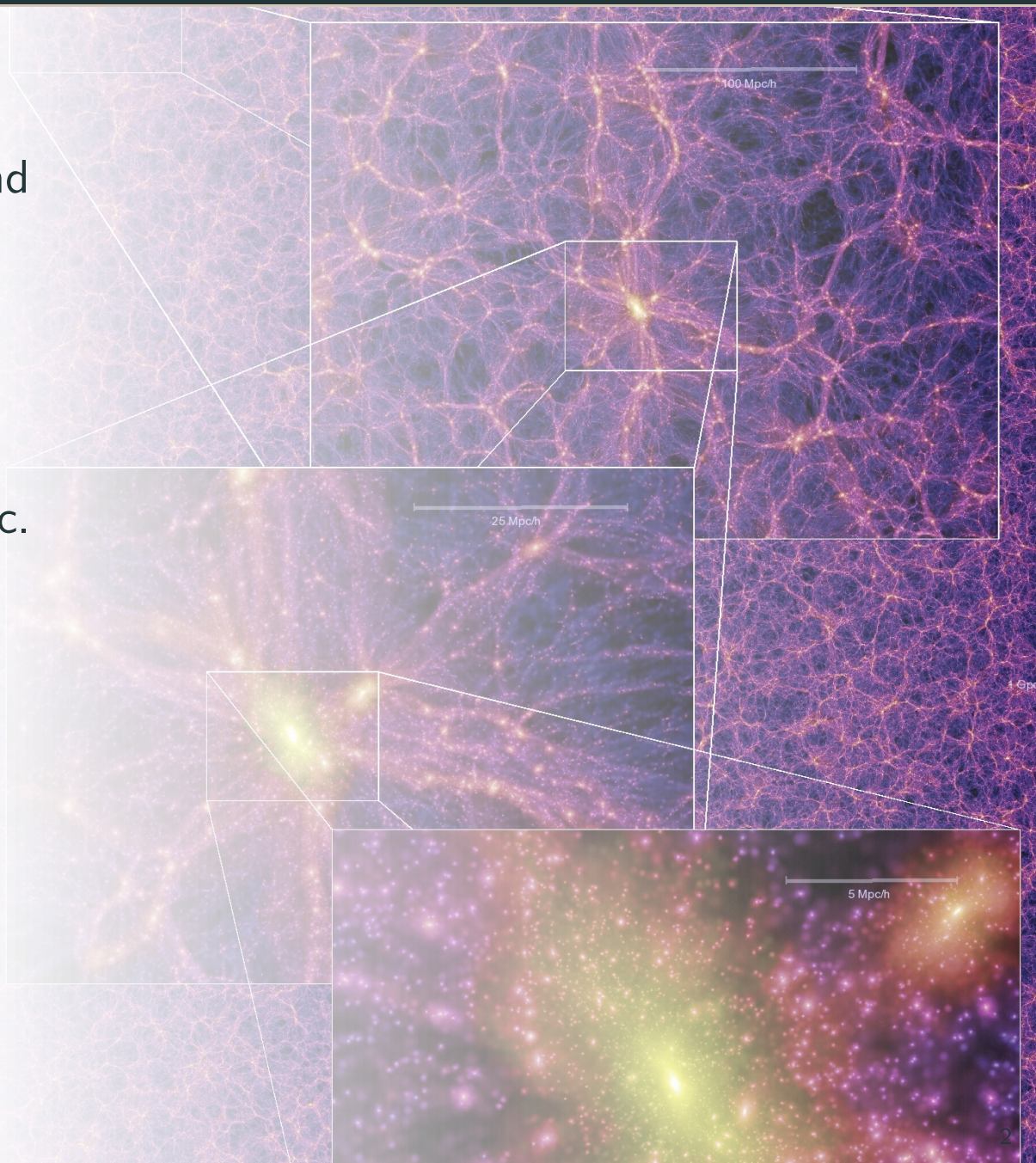

The Kinematic Dipole

- Imprinted on the CMB is a dipole ($\Delta T/T \approx 10^{-3}$).

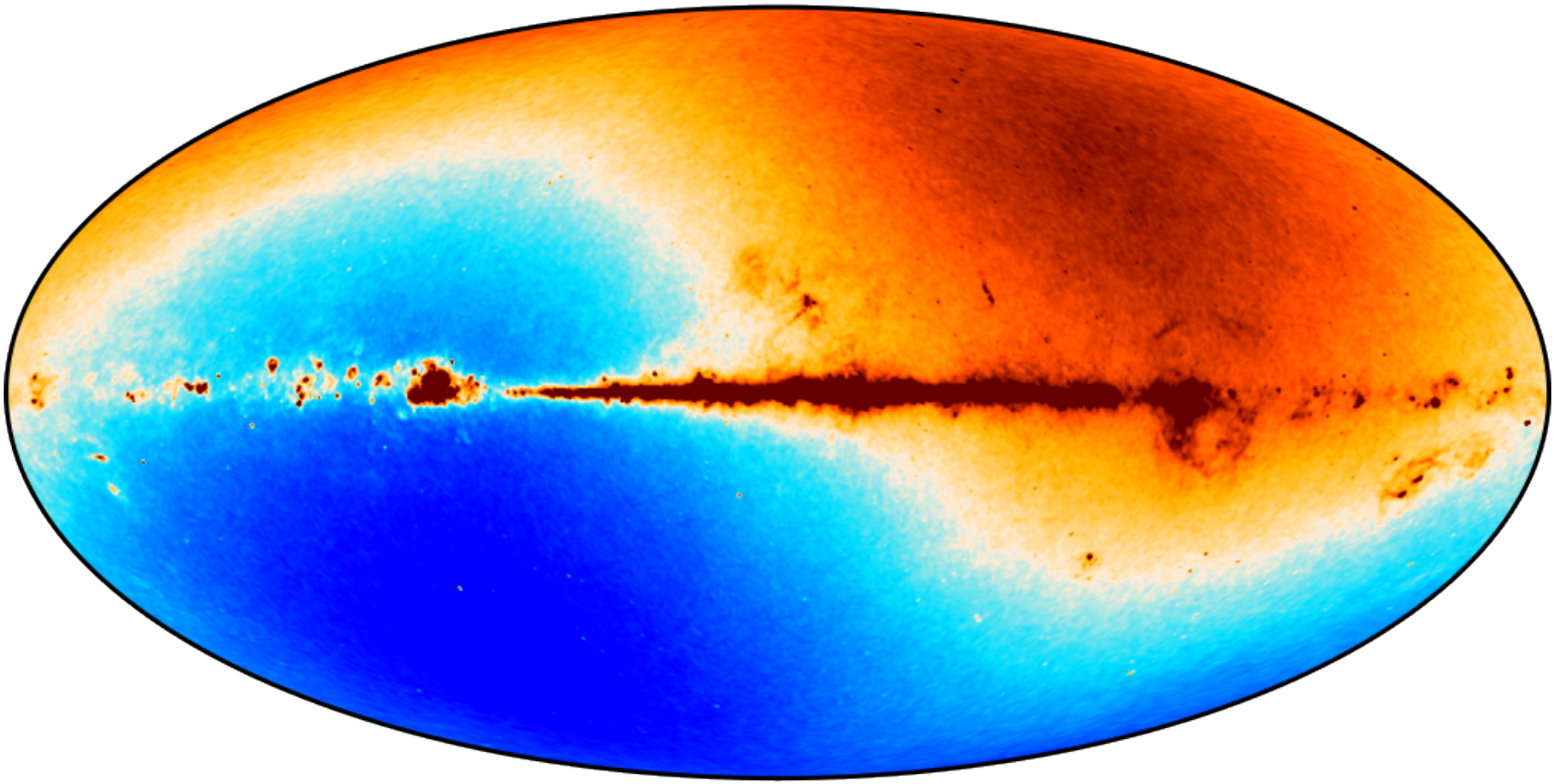

Figure 1: CMB temperature map (Galactic coordinates; kinematic dipole and Galactic contamination included; BeyondPlanck). ★: dipole direction.

The Kinematic Dipole

- Imprinted on the CMB is a dipole ($\Delta T/T \approx 10^{-3}$).
- This is thought to be *kinematic* in origin.

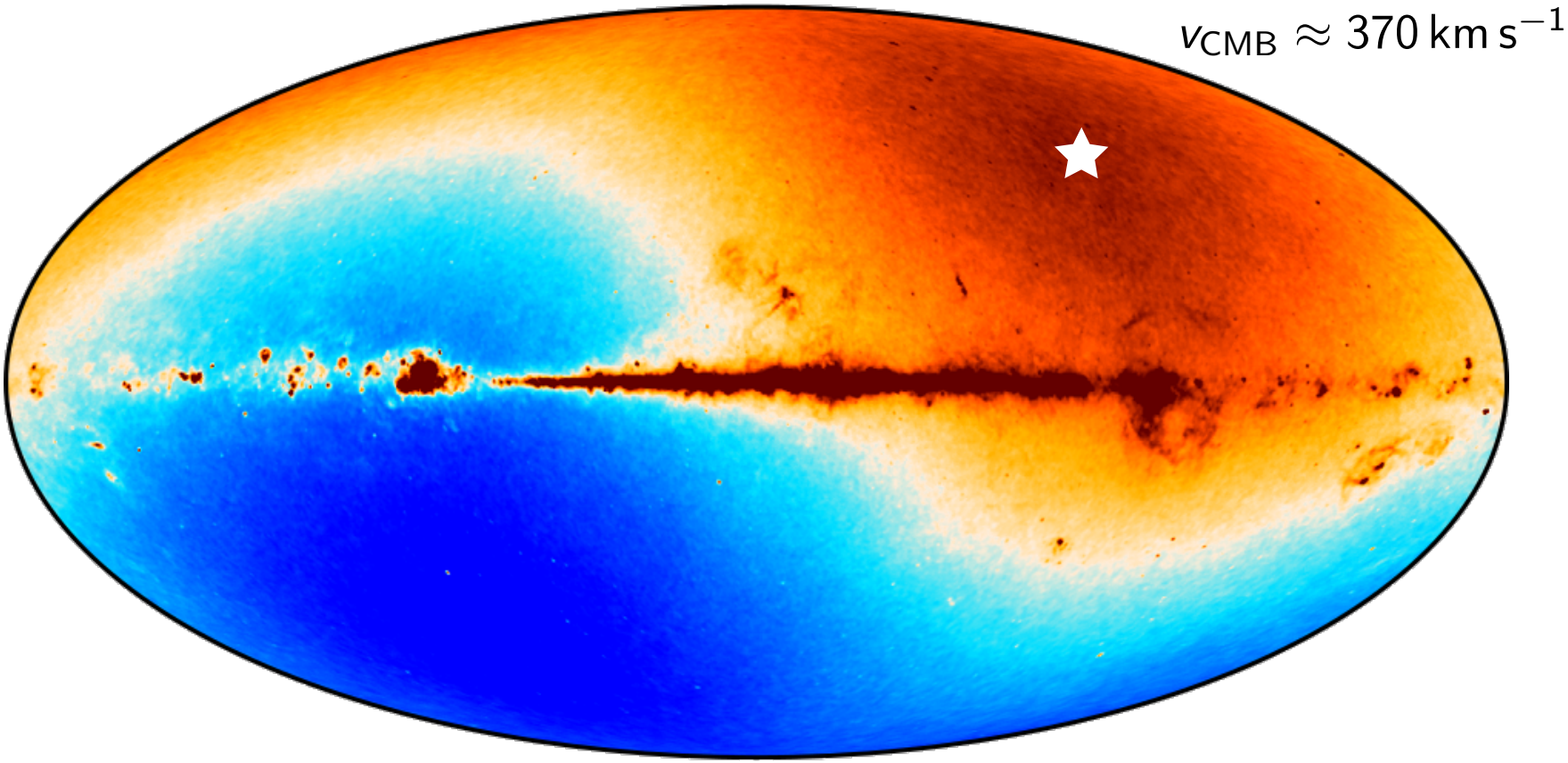

Figure 1: CMB temperature map (Galactic coordinates; kinematic dipole and Galactic contamination included; BeyondPlanck). ★: dipole direction.

The Kinematic Dipole

- Imprinted on the CMB is a dipole ($\Delta T/T \approx 10^{-3}$).
- This is thought to be *kinematic* in origin.

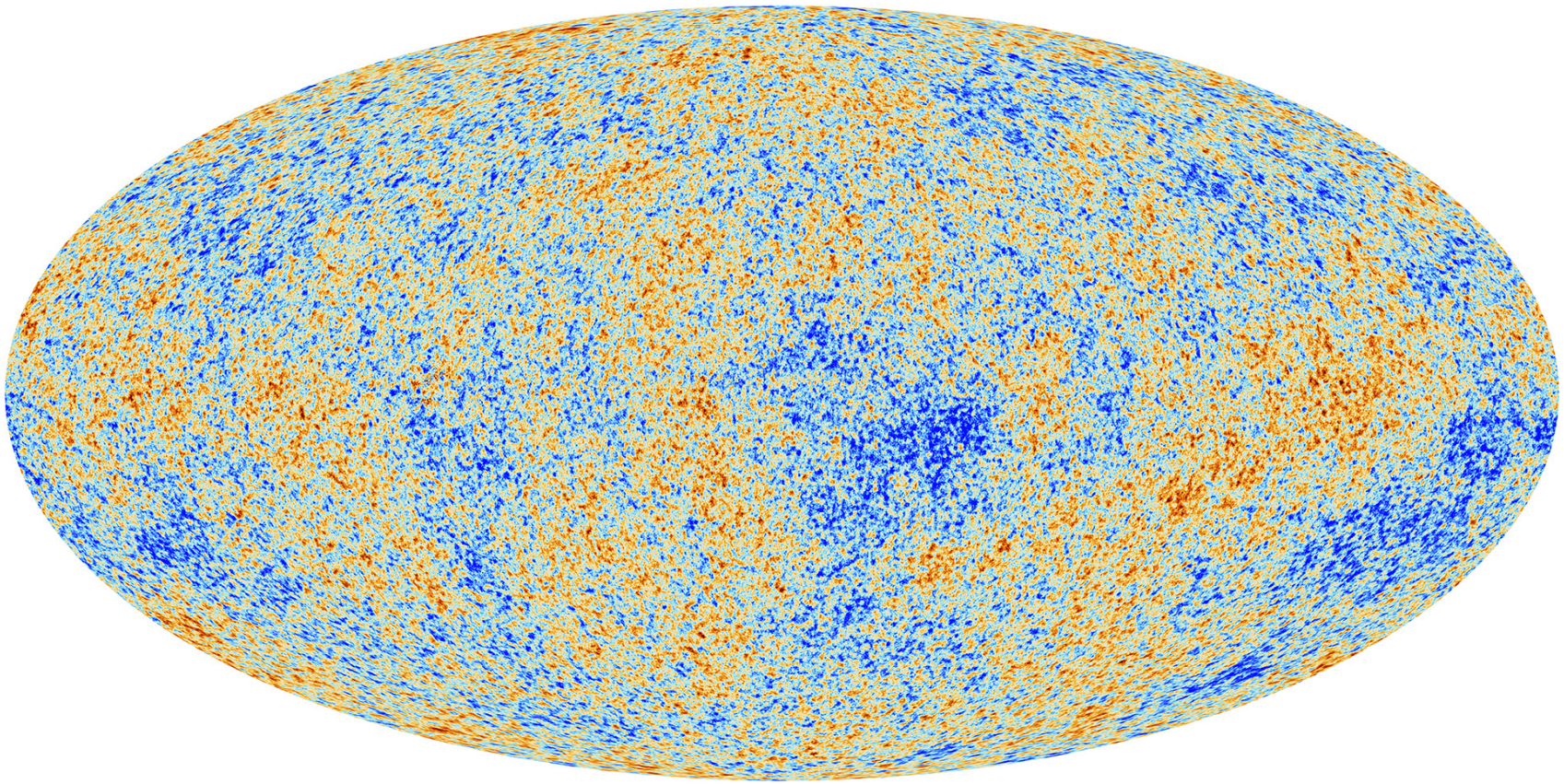

Figure 1: CMB temperature map (dipole excluded; Planck).

The Ellis & Baldwin (1984) Dipole

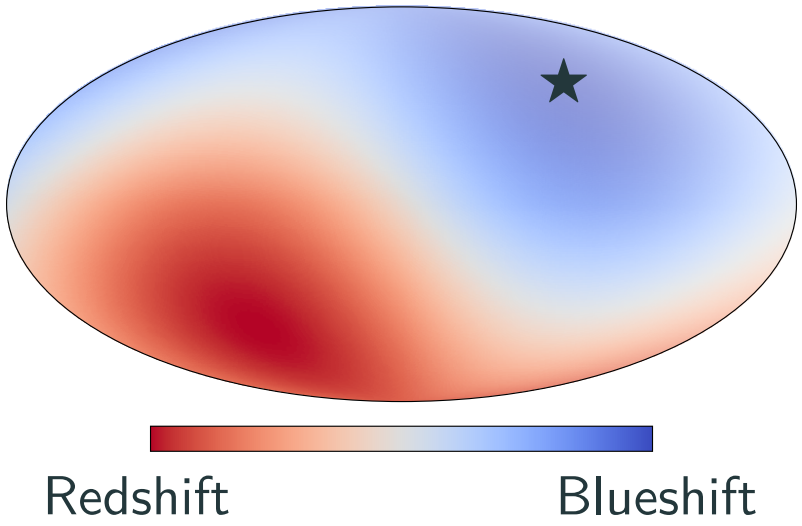

Based on special relatavistic arguments, our motion induces a dipole in source density.

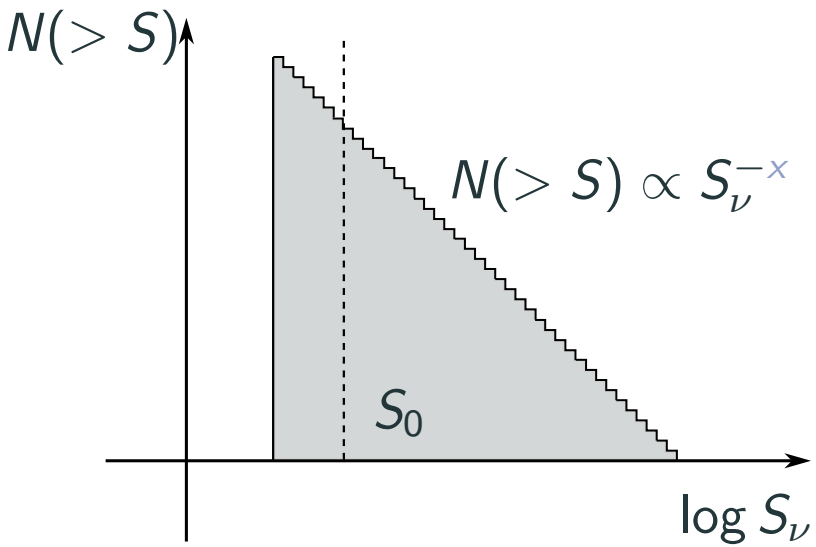

The Ellis & Baldwin (1984) Dipole

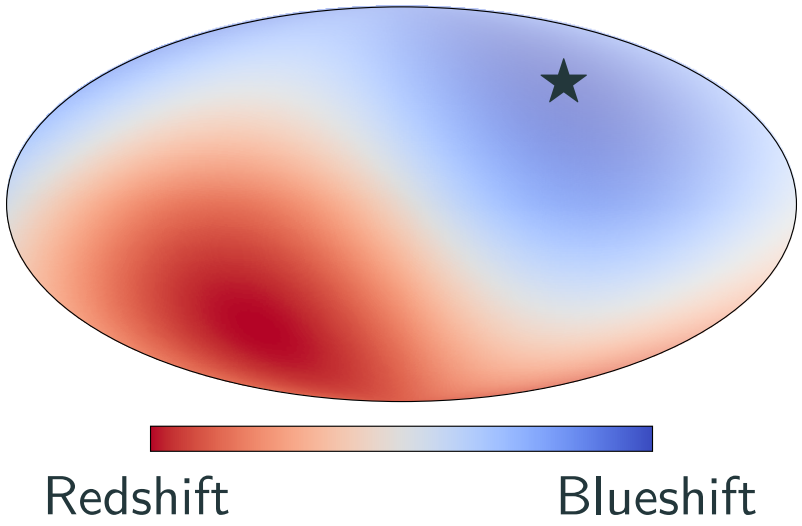

Based on special relatavistic arguments, our motion induces a dipole in source density.

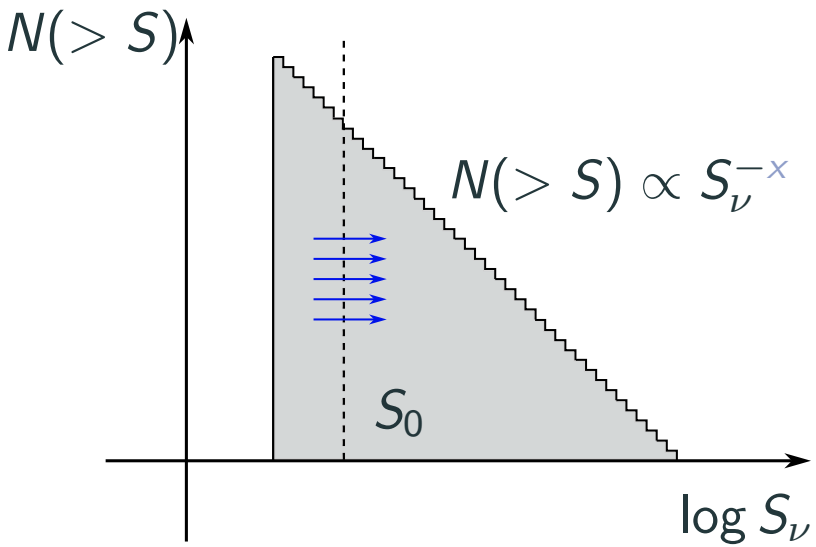

The Ellis & Baldwin (1984) Dipole

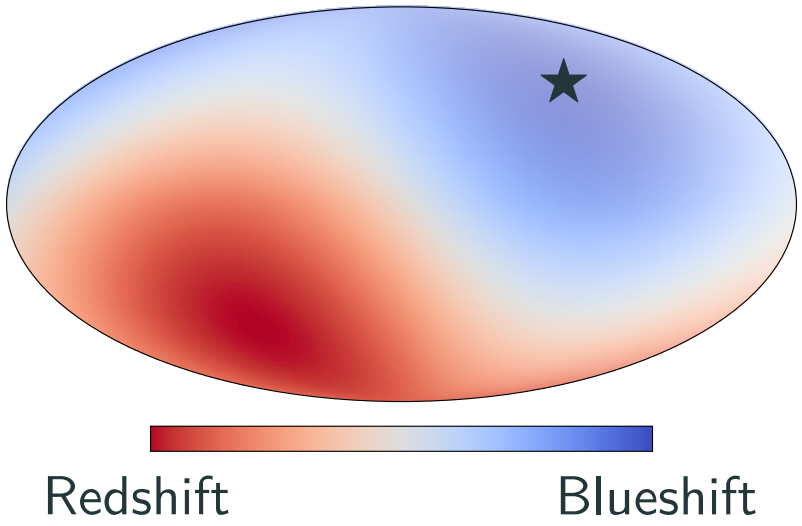

Based on special relatavistic arguments, our motion induces a dipole in source density.

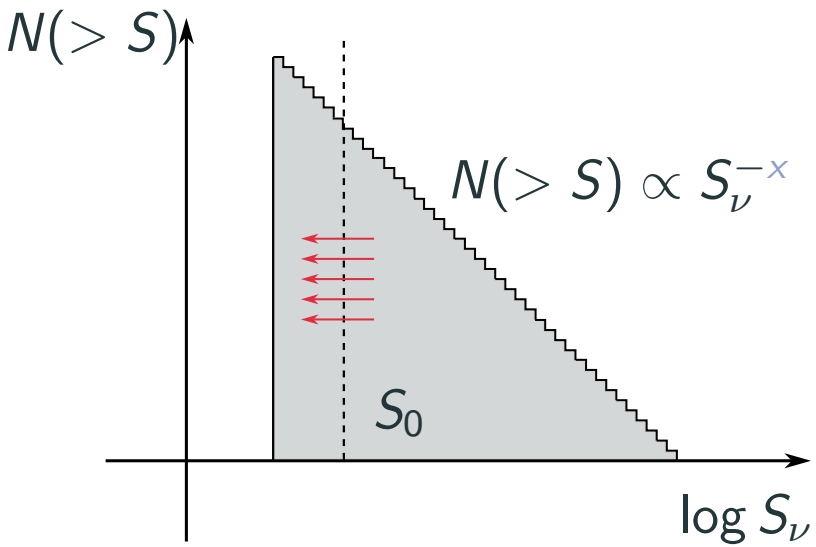

The Ellis & Baldwin (1984) Dipole

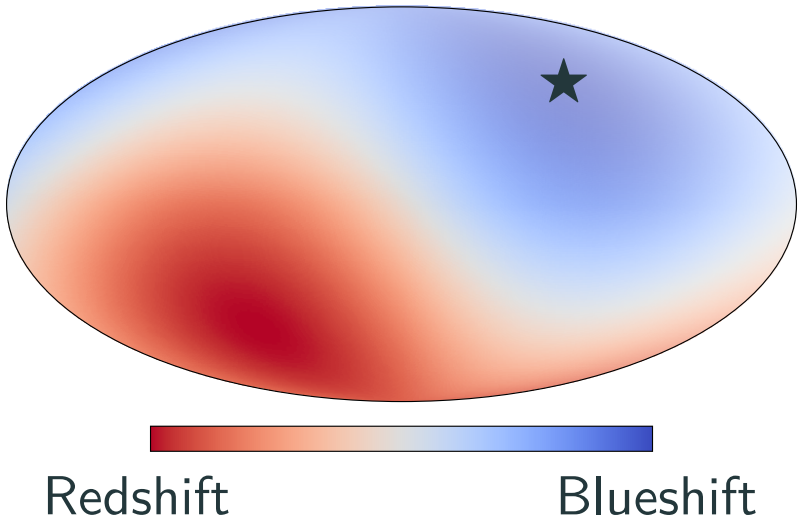

Based on special relatavistic arguments, our motion induces a dipole in source density.

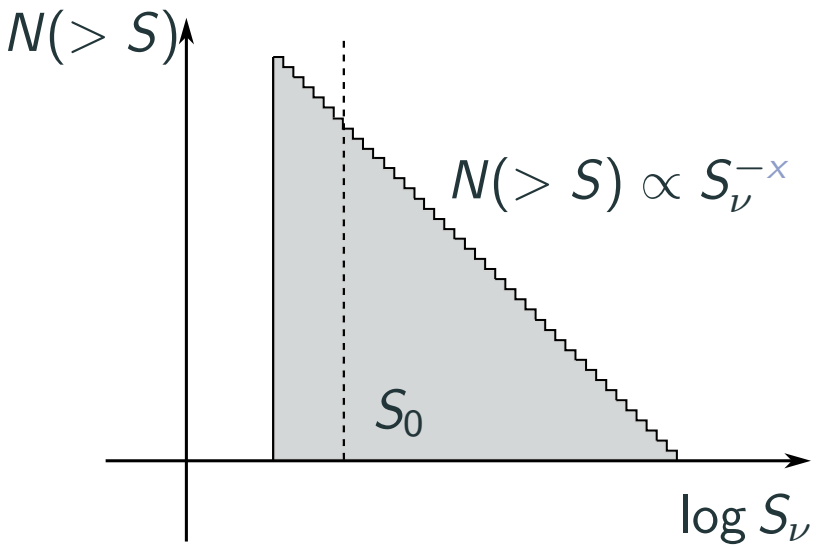

The Ellis & Baldwin (1984) Dipole

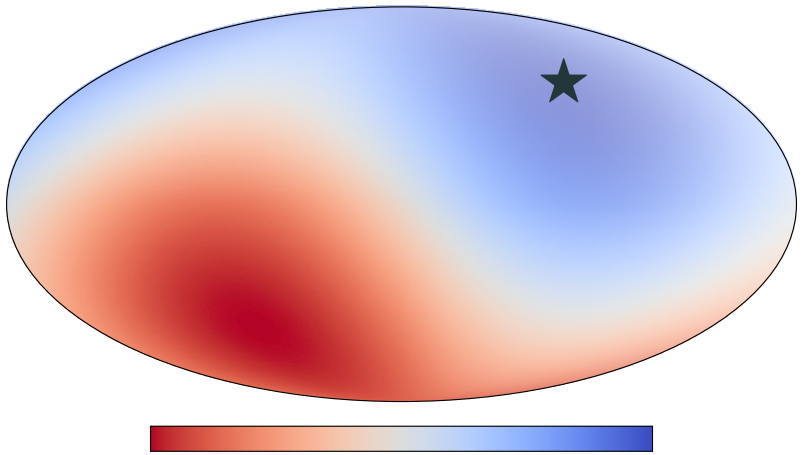

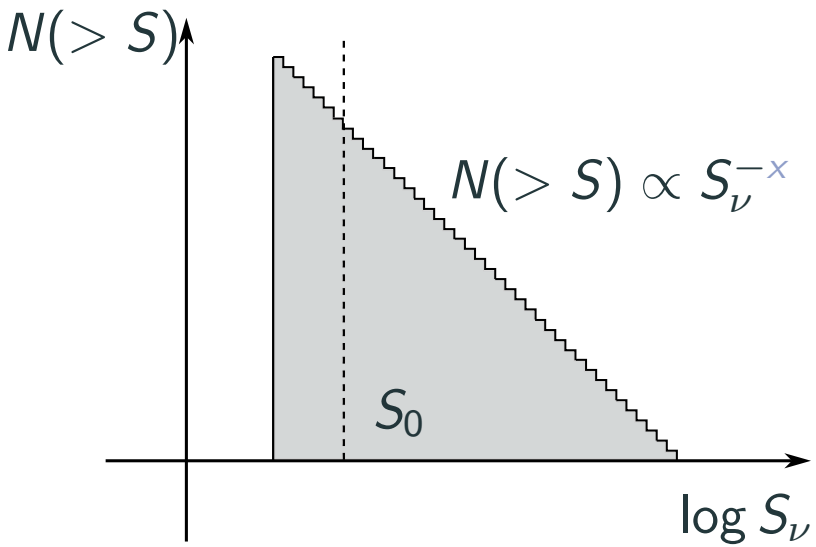

Based on special relatavistic arguments, our motion induces a dipole in source density.

The anticipated dipole amplitude:

$$\mathcal{D}_{\mathrm{CMB}} = [2 + x\,(1 + \alpha)]\,\frac{v_{\mathrm{CMB}}}{c}.$$

The Ellis & Baldwin (1984) Dipole

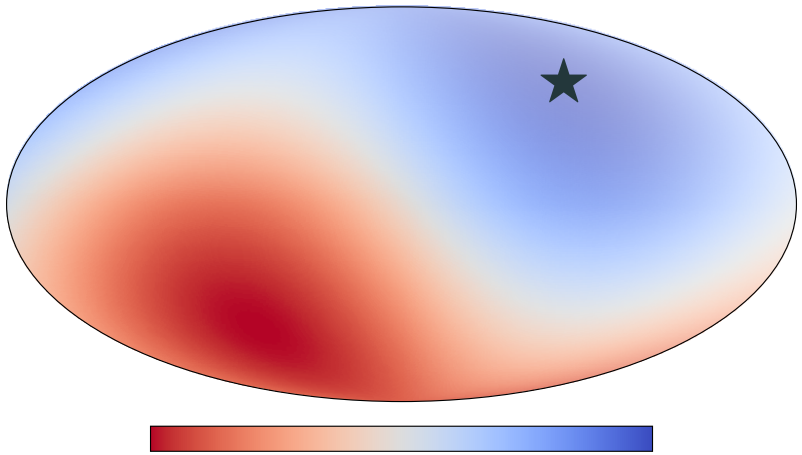

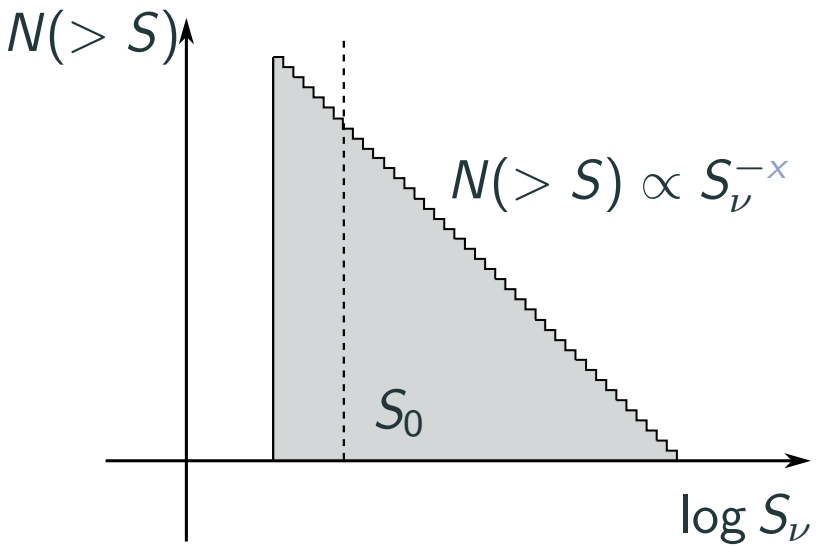

Based on special relatavistic arguments, our motion induces a dipole in source density.

The anticipated dipole amplitude:

$$\mathcal{D}_{\mathrm{CMB}} = [2 + x\,(1 + \alpha)]\,\frac{v_{\mathrm{CMB}}}{c}.$$

Typical values are 0.004 – 0.007. This is a *0.5% effect!*

The Dipole Tension

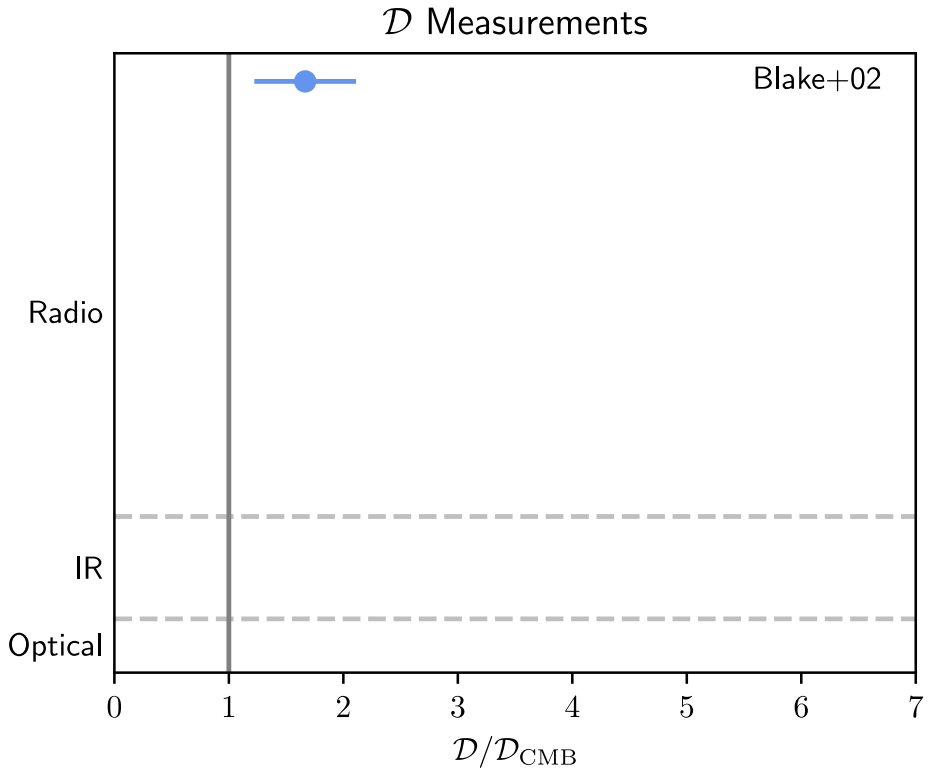

The Dipole Tension

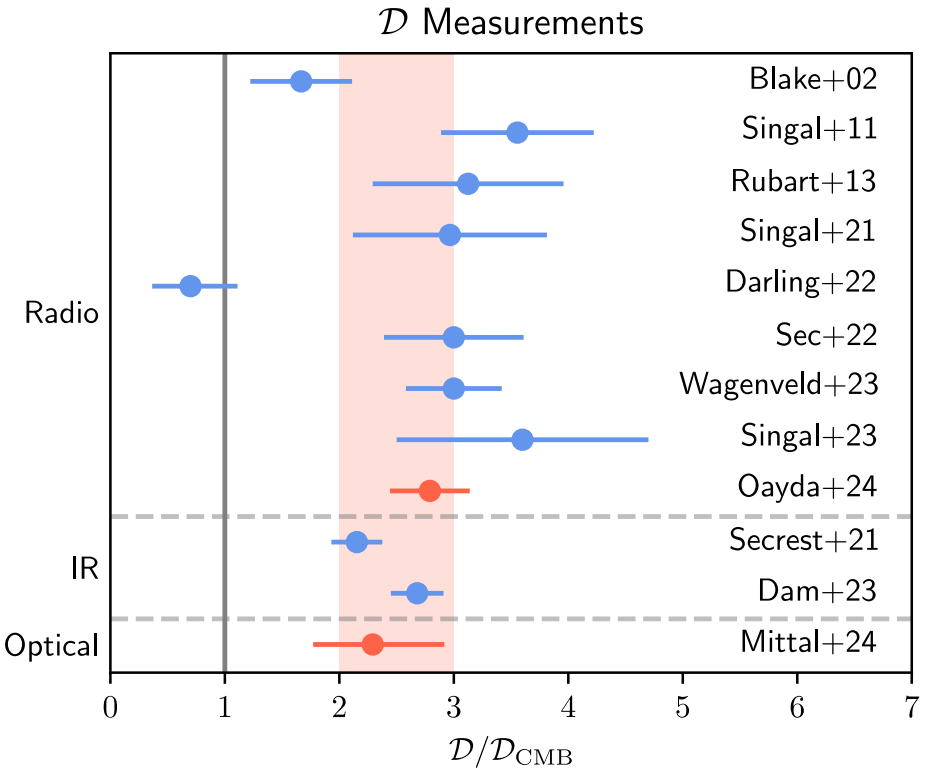

Figure 2: *Top:* Literature values for $\mathcal{D}$ (1σ); our studies in red. *Right:* Dipole direction results from our studies.

The Dipole Tension

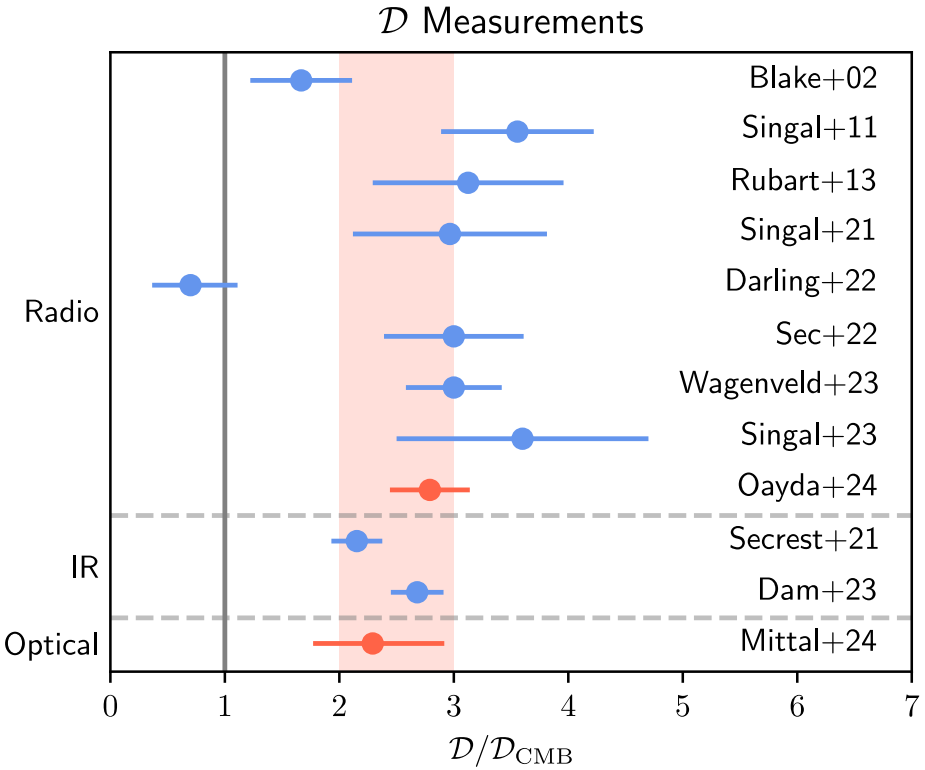

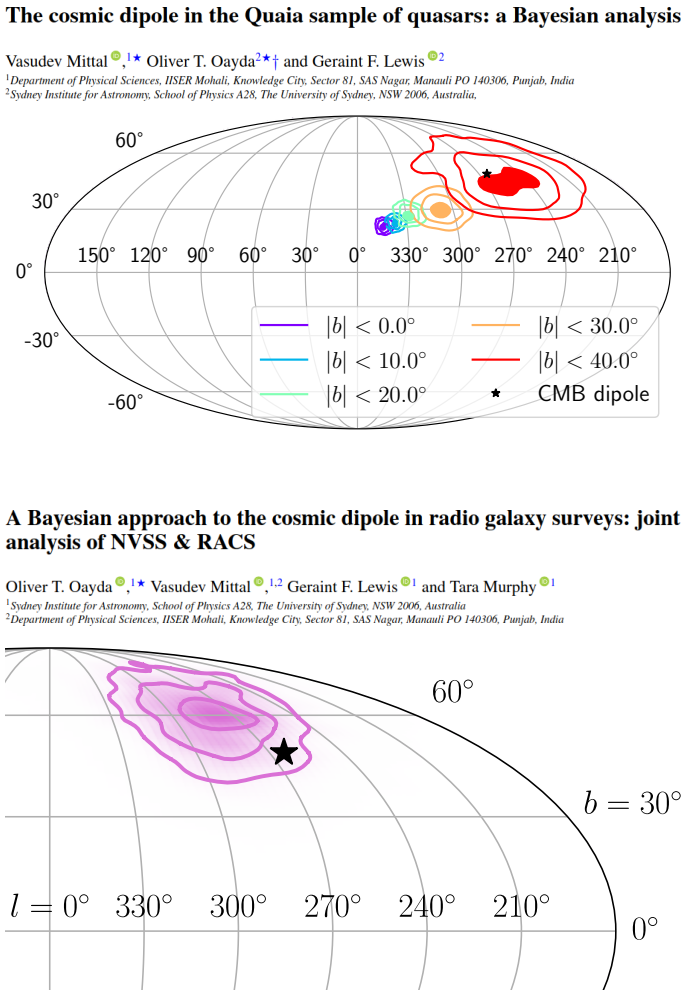

Figure 2: *Top:* Literature values for $\mathcal{D}$ (1σ); our studies in red. *Right:* Dipole direction results from our studies.

Results of Mittal, Oayda & Lewis (2024) — Optical

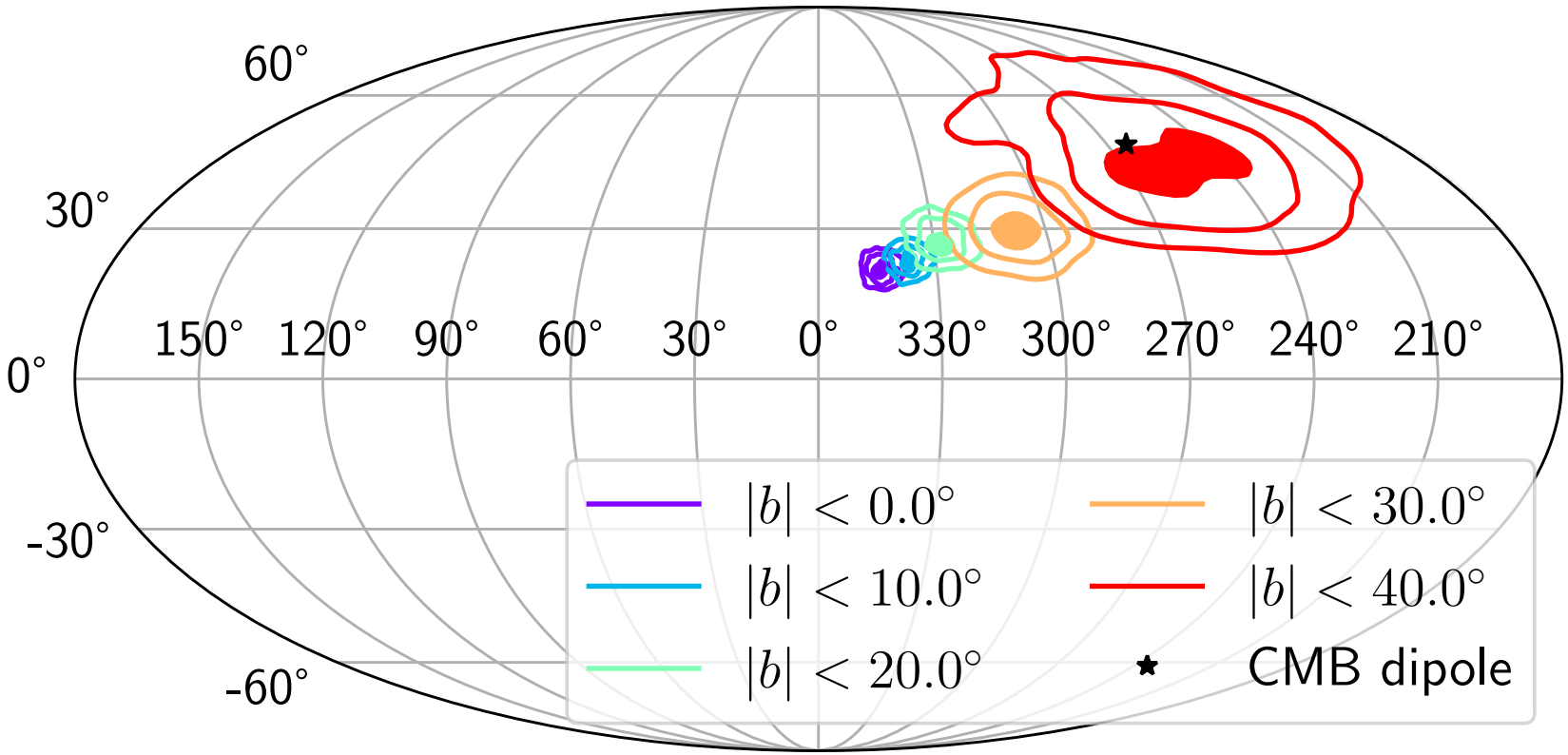

Amplitude $\mathcal{D}$ (10^{-3})	37^{+4}_{-4}	34^{+4}_{-4}	25^{+5}_{-5}	17^{+6}_{-6}	11^{+6}_{-5}	5★

Figure 3: Results from Quaia low ($G < 20.0$) as in Mittal et al. (2024). *Top:* projection of marginal posterior for dipole direction onto the sky. *Bottom:* 2σ credible interval for dipole amplitude by mask choice.

Results of Wagenveld et al. (2023) — Radio

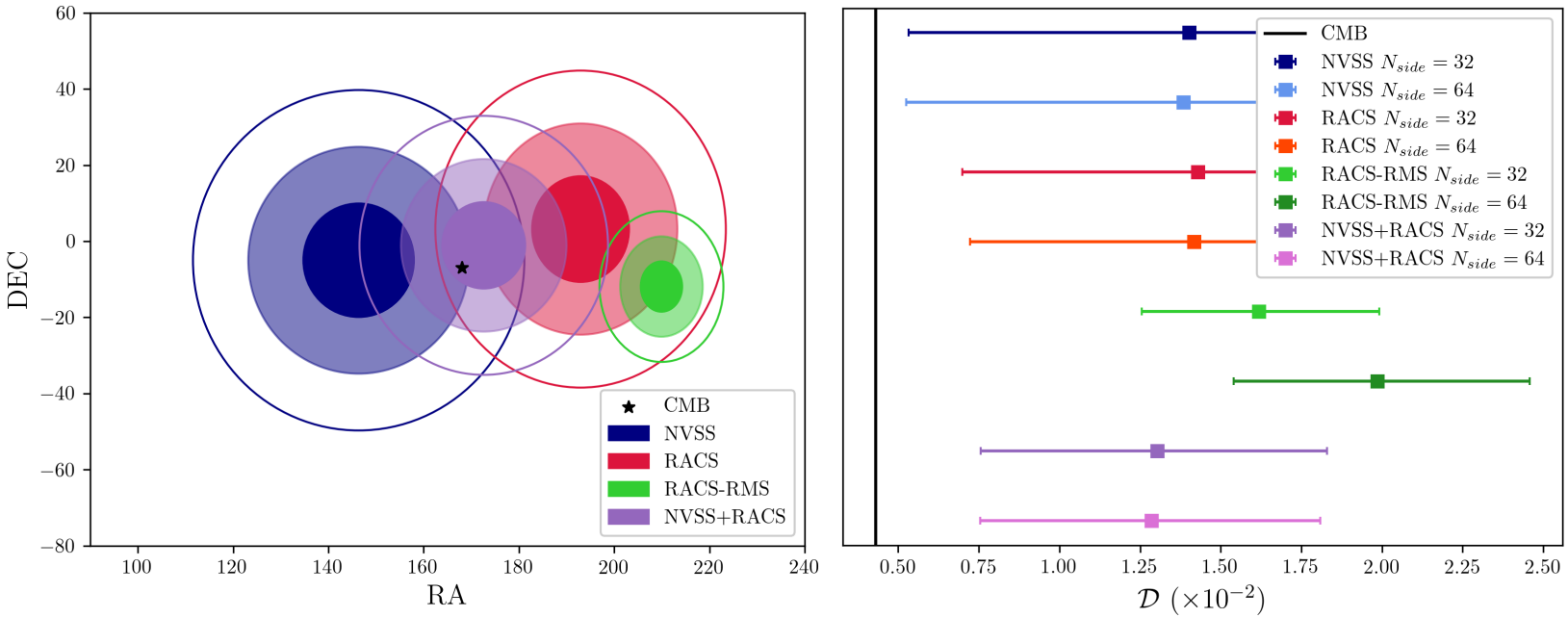

Figure 4: Results of Wagenveld et al. (2023) also point towards an excessive dipole amplitude (but consistent direction).

- '**W23**' — used as prior likelihood later.
- We also analysed NVSS and RACS-low, but with a different approach.

What is going on here? Is this a genuine tension or are there systematics?

Analysis

Samples We Tested

NVSS (NRAO VLA Sky Survey): 1993–97, 1.4 GHz, northern sky.

RACS-low (Rapid Australian SKA Pathfinder Continuum Survey): 2019–20, 887.5 MHz, southern sky.

Figure 5: *Top:* VLA in New Mexico (credit: NRAO). *Bottom:* Australian SKA Pathfinder in Western Australia (credit: CSIRO).

Some Systematic Effects

Some issues to consider:

Some Systematic Effects

Some issues to consider:

- Catalogue completeness at some S_ν.

Some Systematic Effects

Some issues to consider:

- Catalogue completeness at some S_ν.
- Declination-dependent systematics.

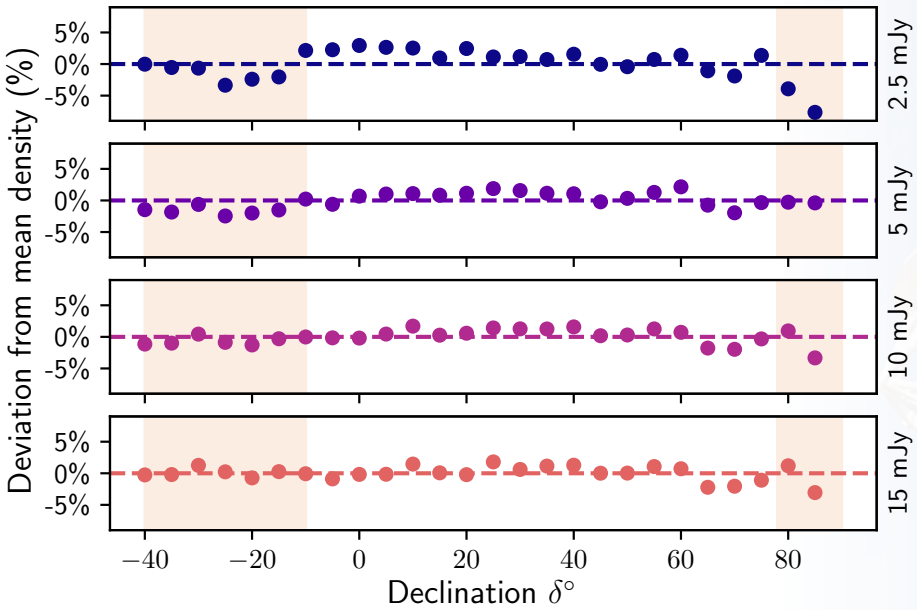

Figure 6: Deviation from mean source density by $\delta°$ (NVSS). *Shaded brown:* DnC config.

Some Systematic Effects

Some issues to consider:

- Catalogue completeness at some S_ν.
- Declination-dependent systematics.
- Contamination from the Galactic plane and bright radio sources.

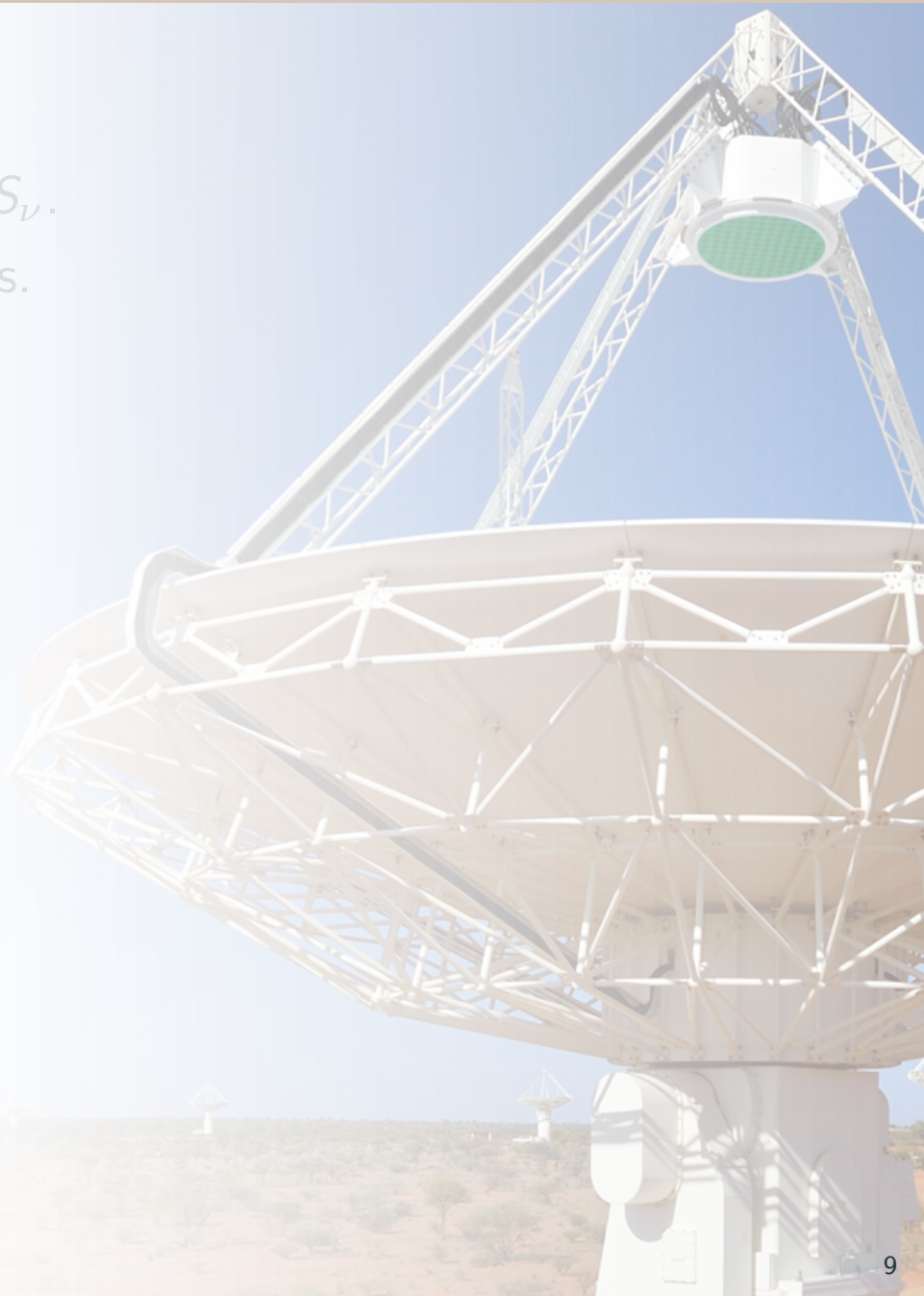

Some Systematic Effects

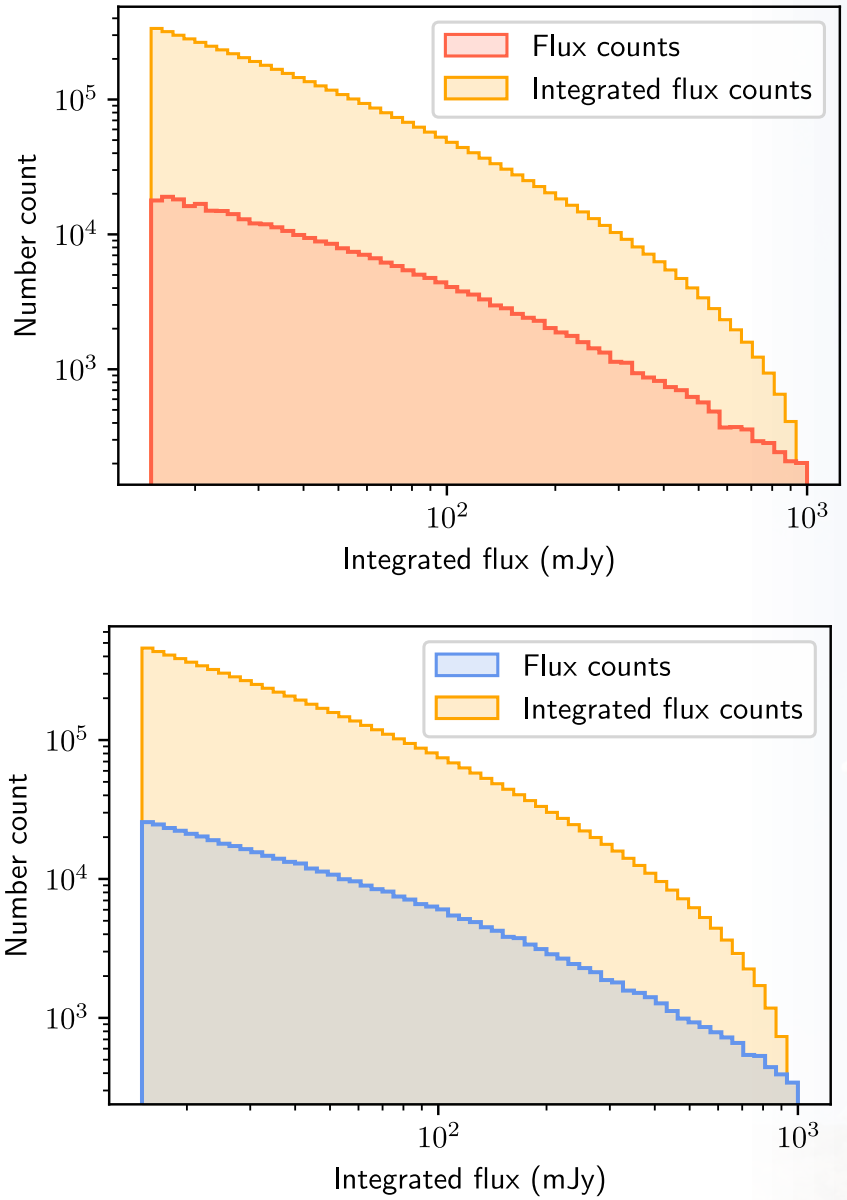

Figure 6: Flux density distribution for NVSS and RACS-low.
$15\,\text{mJy} < S_{\text{int.}} < 1000\,\text{mJy}$.

Preparing NVSS & RACS

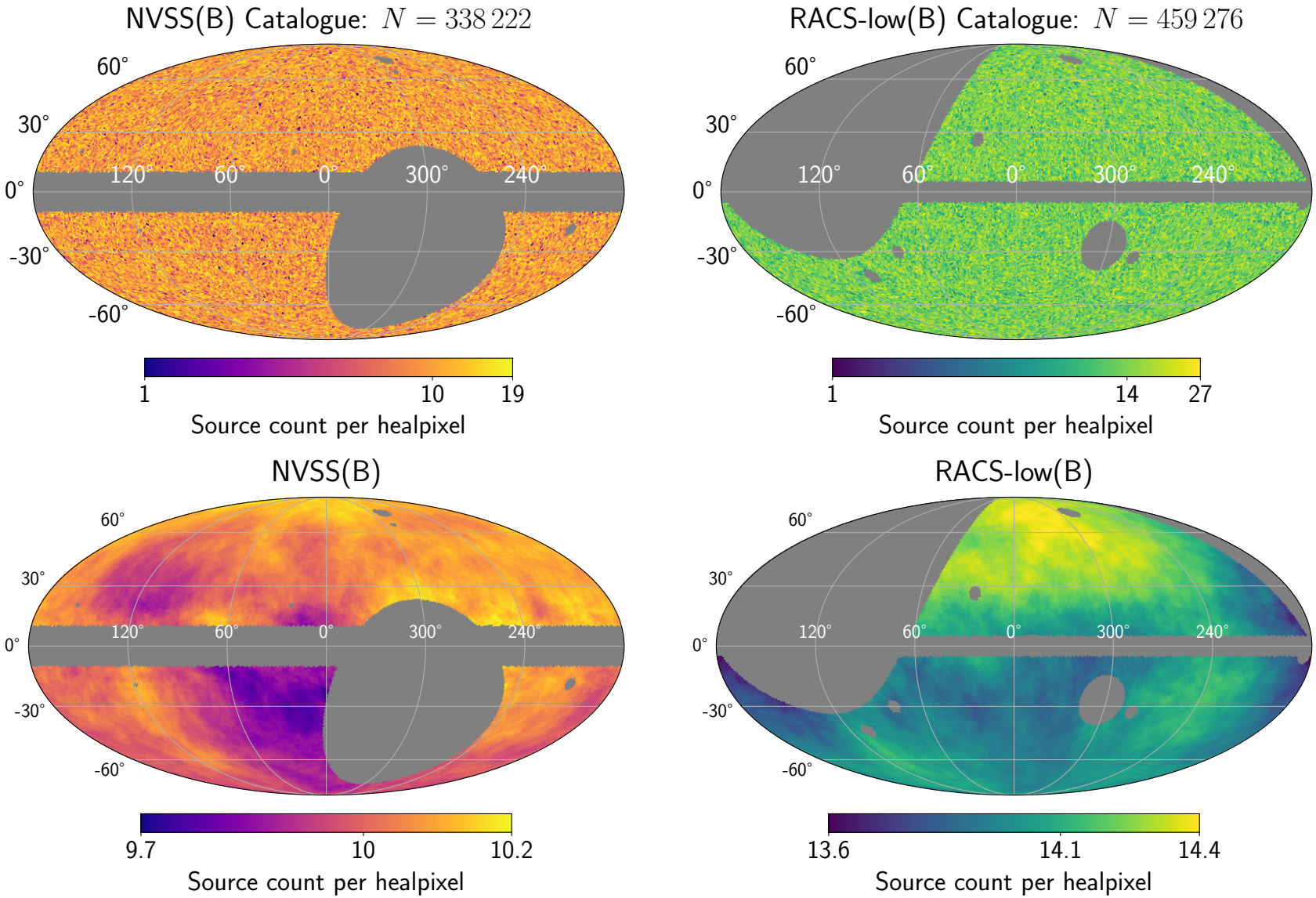

Figure 7: NVSS and RACS-low samples in Galactic coordinates binned into healpixels. *Top:* Raw density maps. *Bottom:* Smoothed density maps.

Statistics: Bayesian Inference

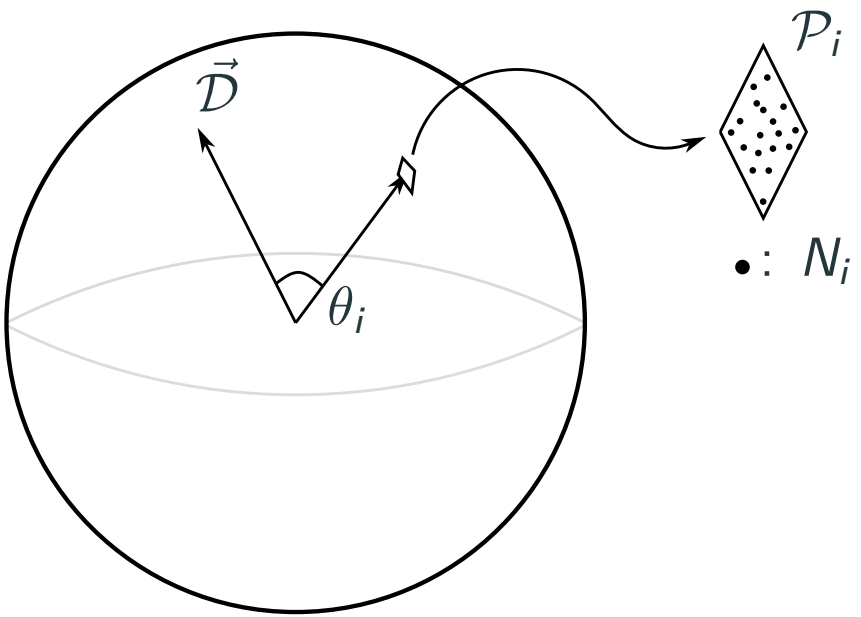

Figure 8: Schematic of pixel $\mathcal{P}_i$ on the celestial sphere with N_i sources $(\cdot)$ near dipole vector $\vec{\mathcal{D}}$.

Dipole vector $\vec{\mathcal{D}}$ is a free parameter.

Statistics: Bayesian Inference

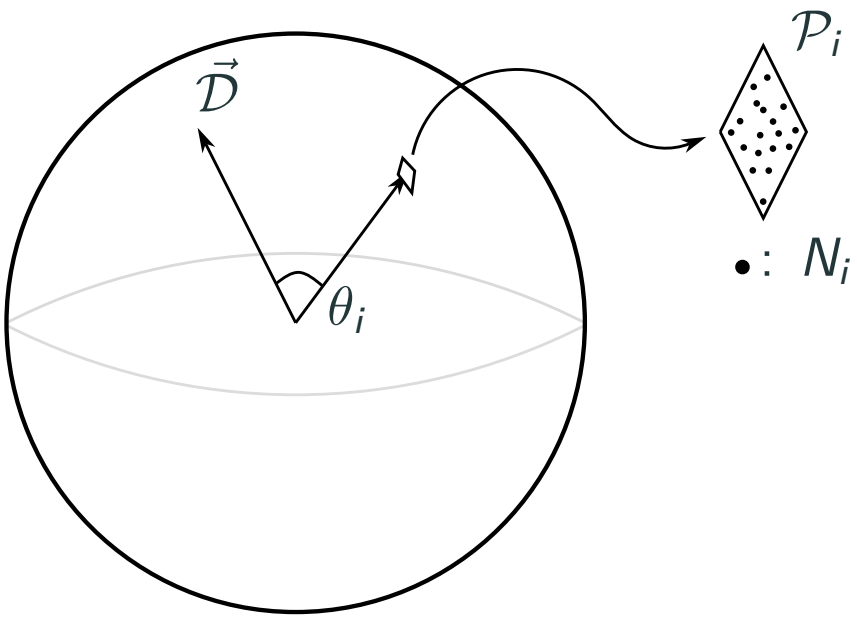

Figure 8: Schematic of pixel $\mathcal{P}_i$ on the celestial sphere with N_i sources $(\cdot)$ near dipole vector $\vec{\mathcal{D}}$.

Dipole vector $\vec{\mathcal{D}}$ is a free parameter.

- Pixel $\mathcal{P}_i$ has N_i sources.

Statistics: Bayesian Inference

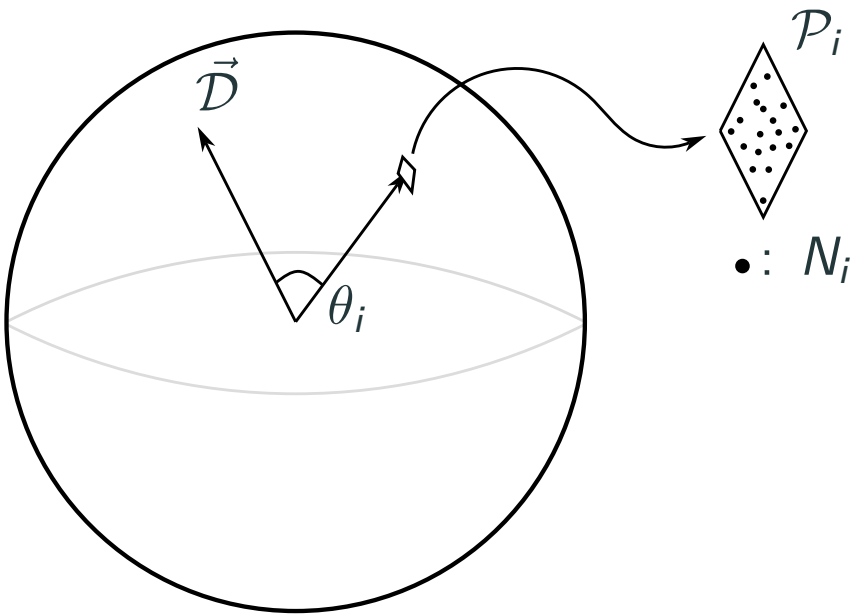

Figure 8: Schematic of pixel $\mathcal{P}_i$ on the celestial sphere with N_i sources $(\cdot)$ near dipole vector $\vec{\mathcal{D}}$.

Dipole vector $\vec{\mathcal{D}}$ is a free parameter.

- Pixel $\mathcal{P}_i$ has N_i sources.
- $\mathbb{E}[N_i] = \bar{N}(1 + \mathcal{D}\cos\theta_i)$

Statistics: Bayesian Inference

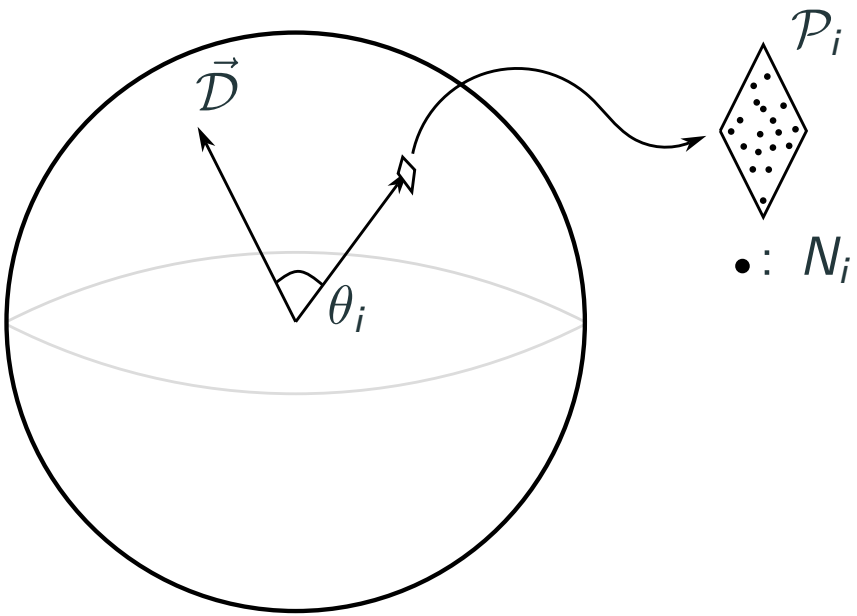

Figure 8: Schematic of pixel $\mathcal{P}_i$ on the celestial sphere with N_i sources $(\cdot)$ near dipole vector $\vec{\mathcal{D}}$.

Dipole vector $\vec{\mathcal{D}}$ is a free parameter.

- Pixel $\mathcal{P}_i$ has N_i sources.
- $\mathbb{E}[N_i] = \bar{N}(1 + \mathcal{D}\cos\theta_i)$
- Construct a probability map over the sky.

Statistics: Bayesian Inference

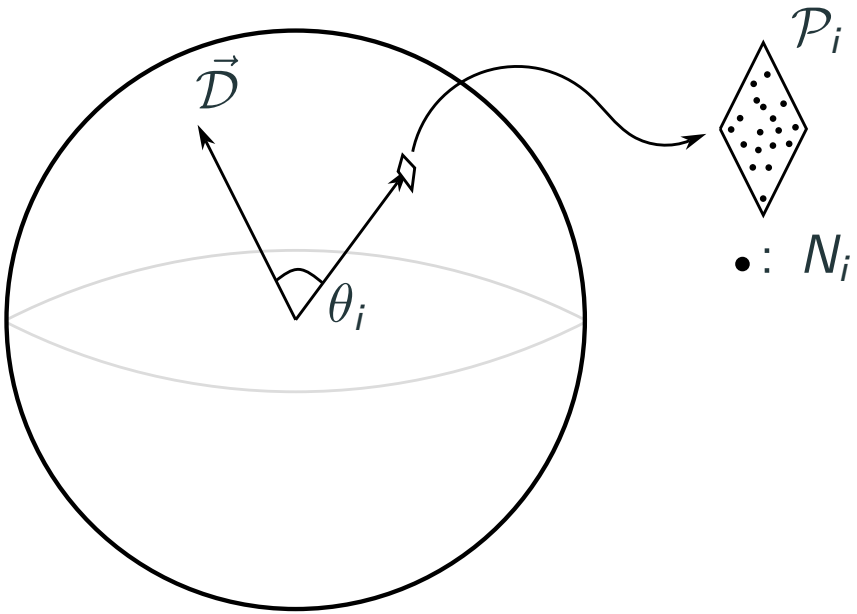

Figure 8: Schematic of pixel $\mathcal{P}_i$ on the celestial sphere with N_i sources $(\cdot)$ near dipole vector $\vec{\mathcal{D}}$.

Dipole vector $\vec{\mathcal{D}}$ is a free parameter.

- Pixel $\mathcal{P}_i$ has N_i sources.
- $\mathbb{E}[N_i] = \bar{N}(1 + \mathcal{D}\cos\theta_i)$
- Construct a probability map over the sky.

Yields a likelihood function $\mathcal{L}$ which we can plug into Bayes' theorem

$$P(\Theta|\mathbf{D}, M) = \frac{\mathcal{L}(\mathbf{D}|\Theta, M)\pi(\Theta|M)}{\mathcal{Z}(\mathbf{D}|M)}.$$

Statistics: Bayesian Inference

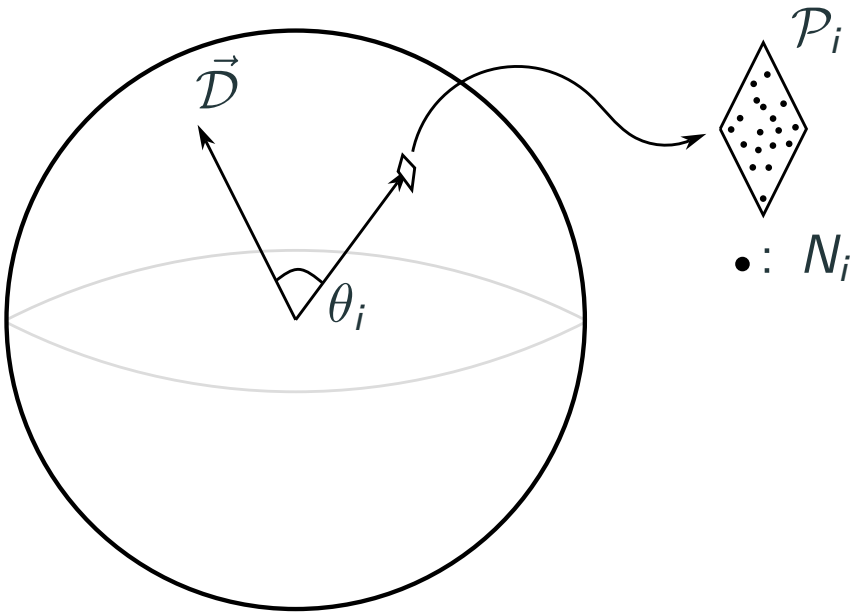

Figure 8: Schematic of pixel $\mathcal{P}_i$ on the celestial sphere with N_i sources $(\cdot)$ near dipole vector $\vec{\mathcal{D}}$.

Dipole vector $\vec{\mathcal{D}}$ is a free parameter.

- Pixel $\mathcal{P}_i$ has N_i sources.
- $\mathbb{E}[N_i] = \bar{N}(1 + \mathcal{D}\cos\theta_i)$
- Construct a probability map over the sky.

Yields a likelihood function $\mathcal{L}$ which we can plug into Bayes' theorem

$$P(\Theta|\mathbf{D}, M) = \frac{\mathcal{L}(\mathbf{D}|\Theta, M)\pi(\Theta|M)}{\mathcal{Z}(\mathbf{D}|M)}.$$

Use a Bayesian statistical approach to infer posterior probability distribution for $\Theta = \{\mathcal{D}, l, b\}$. Analyse individually and jointly.

Model Comparison

	Short label	Description
M_0	Null	Monopole
M_1	Free dipole	Free $\mathcal{D}$, l, b
M_2	Kinematic velocity	$\mathcal{D}$ fixed and free l, b
M_3	Kinematic direction	l, b fixed and free $\mathcal{D}$
M_4	Kinematic dipole	All parameters fixed to CMB expectation
M_5	W23	$\mathcal{D}$, l, b from Wagenveld et al. (2023)

Table 1: The six models tested and ranked.

Compare models' explanatory power with marginal likelihood $\mathcal{Z}(\mathbf{D}|M)$.

This gives us the Bayes factor $\ln B_{i0} = \ln \mathcal{Z}_i - \ln \mathcal{Z}_0$.

Results

NVSS & RACS: Individual Results

$$\boxed{\mathcal{D}_{\mathrm{CMB}} \approx 0.004}$$

NVSS & RACS: Individual Results

$$\mathcal{D}_{\mathrm{CMB}} \approx 0.004$$

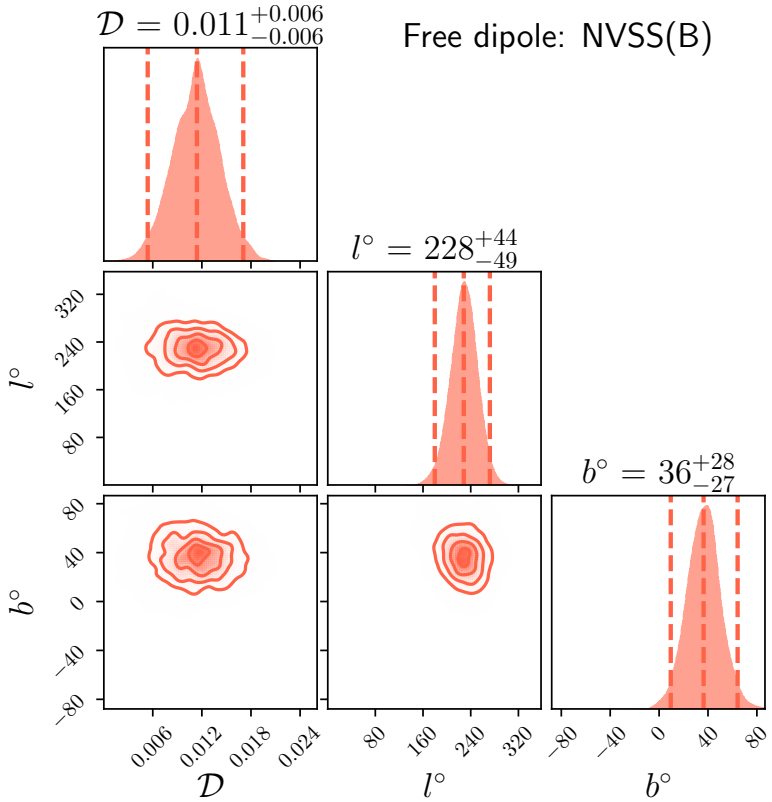

Model		$\ln B_{i0}$
M_1	Free dipole	3.1
M_3	Kin. direction	4.5
M_4	Kin. dipole	4.8

NVSS & RACS: Individual Results

$$\mathcal{D}_{\mathrm{CMB}} \approx 0.004$$

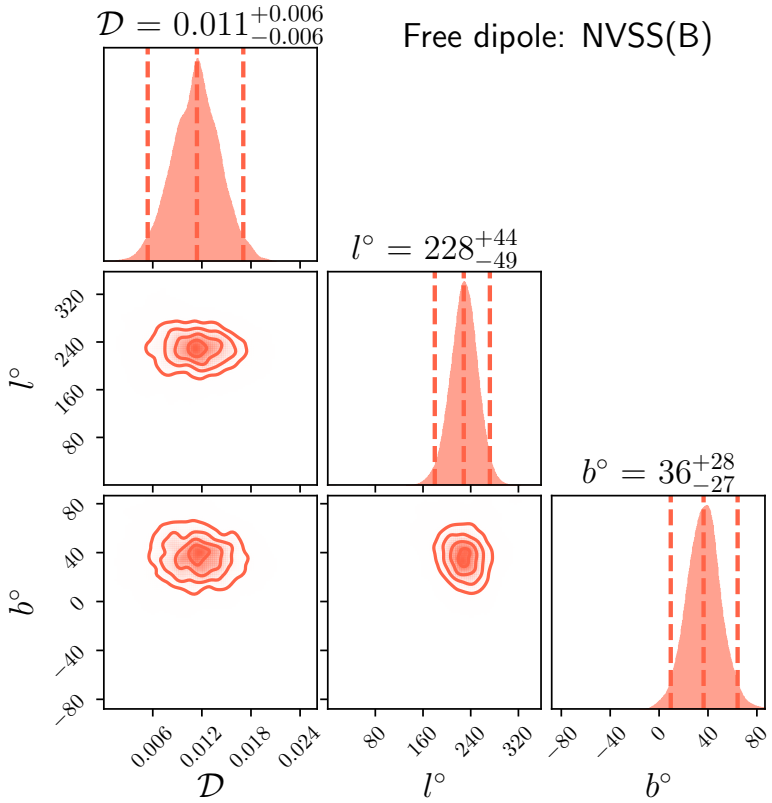

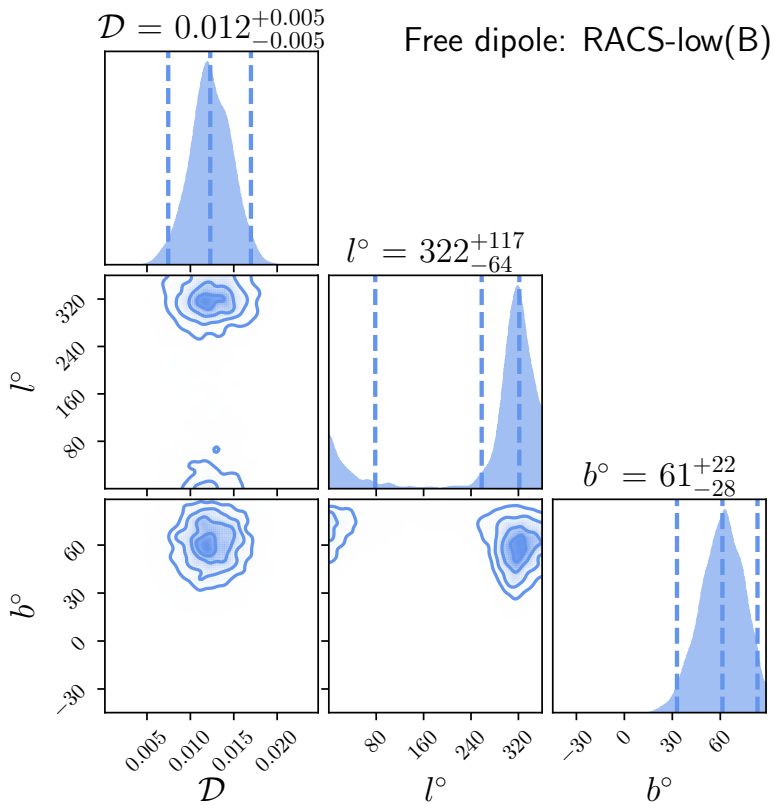

Model		$\ln B_{i0}$
M_1	Free dipole	3.1
M_3	Kin. direction	4.5
M_4	Kin. dipole	4.8

Model		$\ln B_{i0}$
M_1	Free dipole	8.2
M_3	Kin. direction	7.5
M_4	Kin. dipole	6.6

NVSS & RACS: Individual Results

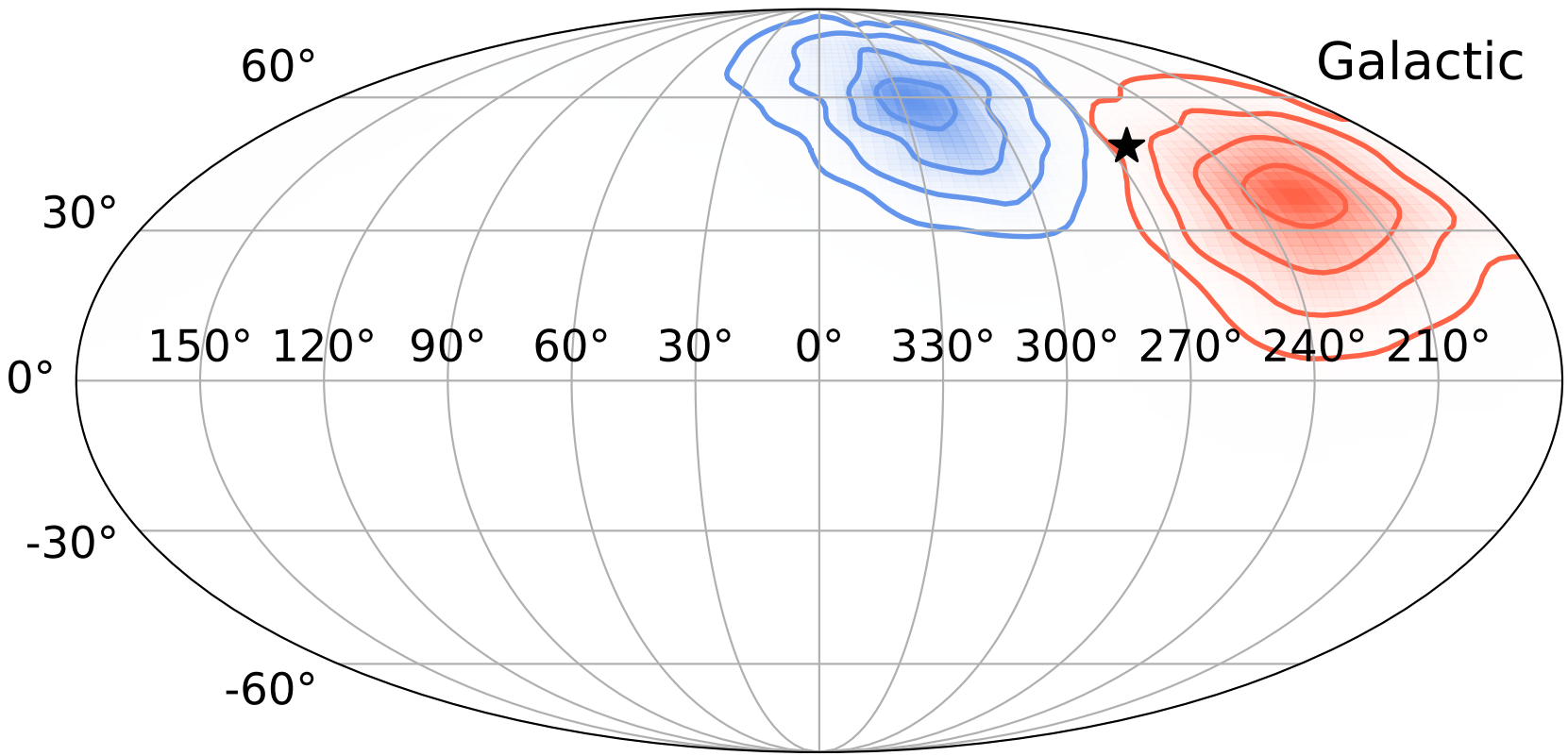

Figure 9: Projection of distribution for l and b onto the sky (Galactic coordinates) for RACS-low and NVSS. ★: CMB dipole.

$$\mathcal{D}_{\text{NVSS}} \approx (11 \pm 6) \times 10^{-3} \qquad \mathcal{D}_{\text{RACS}} \approx (12 \pm 5) \times 10^{-3}$$

Joint Analysis: NVSS + RACS-low

$\boxed{\mathcal{D}_{\mathrm{CMB}} \approx 0.004}$ — $\ln \mathcal{L} = \ln \mathcal{L}_{\mathrm{NVSS}} + \mathcal{L}_{\mathrm{RACS}}$

Joint Analysis: NVSS + RACS-low

$\boxed{\mathcal{D}_{\mathrm{CMB}} \approx 0.004}$ — $\ln \mathcal{L} = \ln \mathcal{L}_{\mathrm{NVSS}} + \mathcal{L}_{\mathrm{RACS}}$

Free dipole: joint

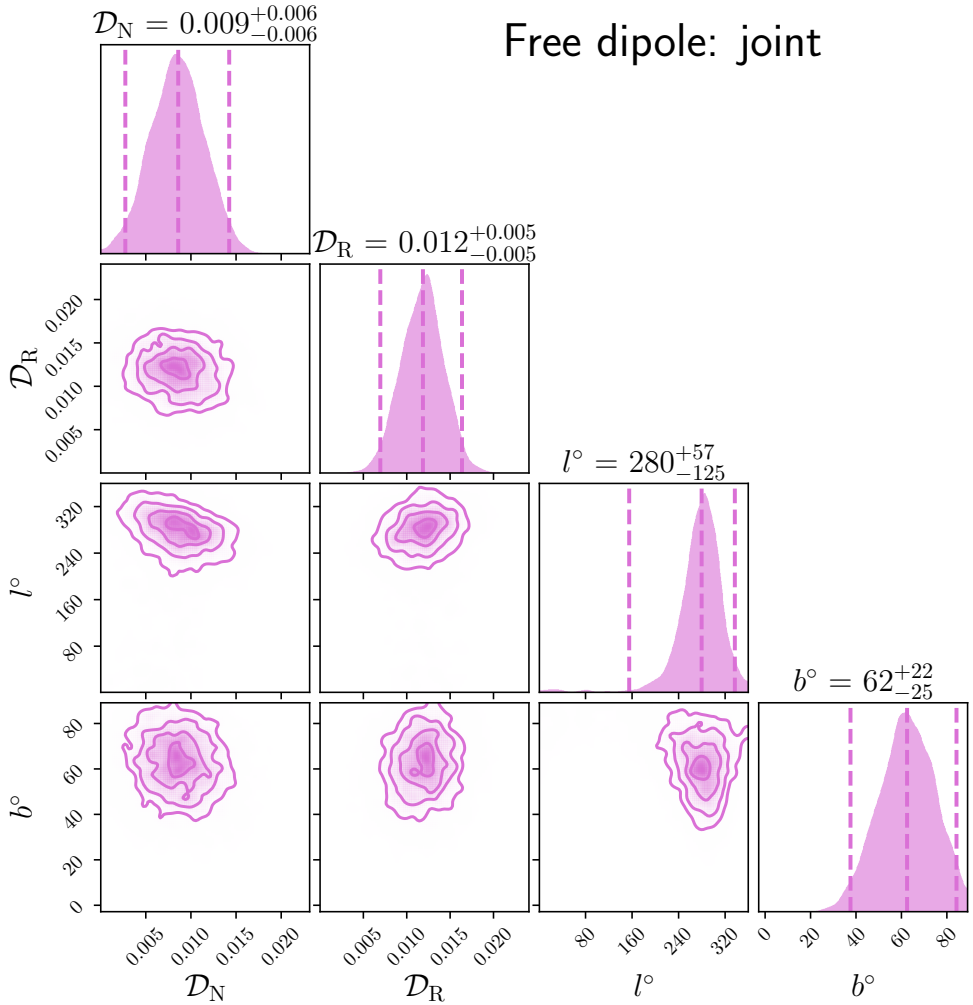

Joint Analysis: NVSS + RACS-low

$\boxed{\mathcal{D}_{\mathrm{CMB}} \approx 0.004}$ — $\ln \mathcal{L} = \ln \mathcal{L}_{\mathrm{NVSS}} + \mathcal{L}_{\mathrm{RACS}}$

Free dipole: joint

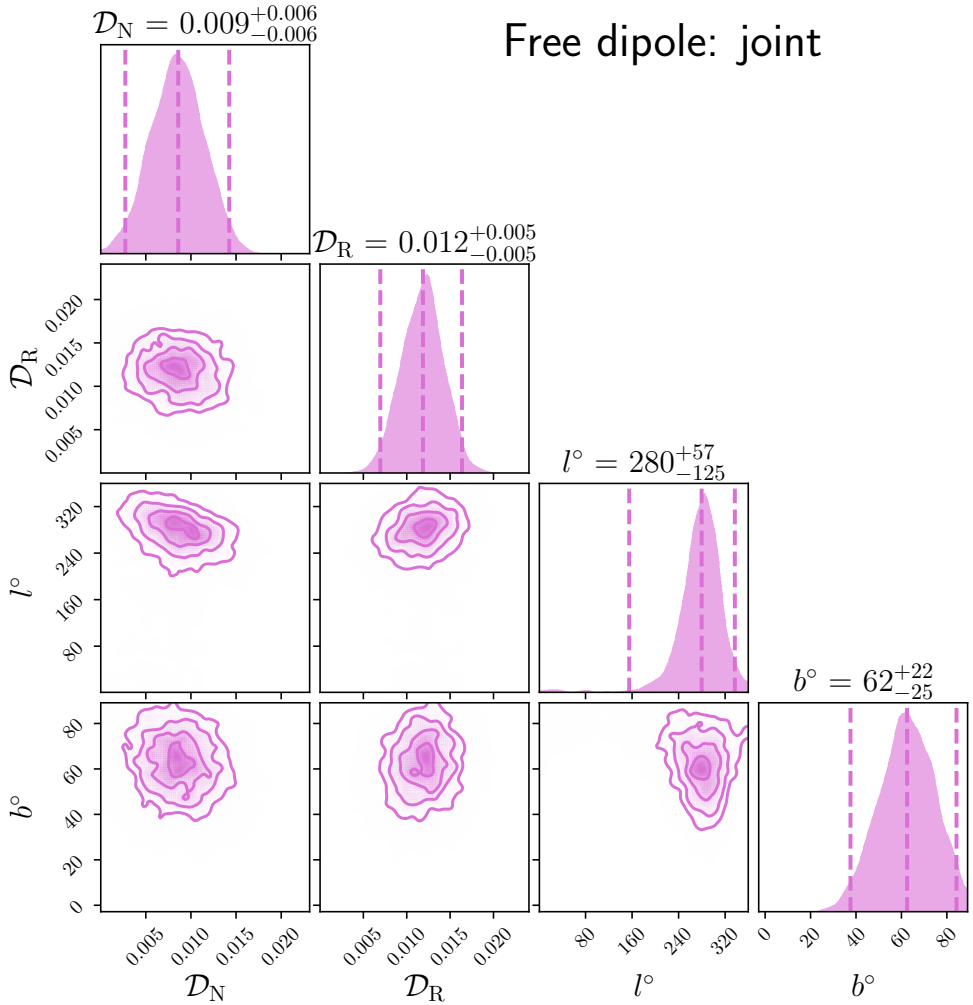

Model		$\ln B_{i0}$
M_3	Kin. dir.	12.1
M_4	Kin. dipole	11.4
M_5	W23	17.1

M_3 (kinematic direction):

$\mathcal{D}_{\mathrm{NVSS}} \approx (10 \pm 5) \times 10^{-3}$

$\mathcal{D}_{\mathrm{RACS}} \approx (11 \pm 5) \times 10^{-3}$

Joint Analysis: Dipole Position Distribution

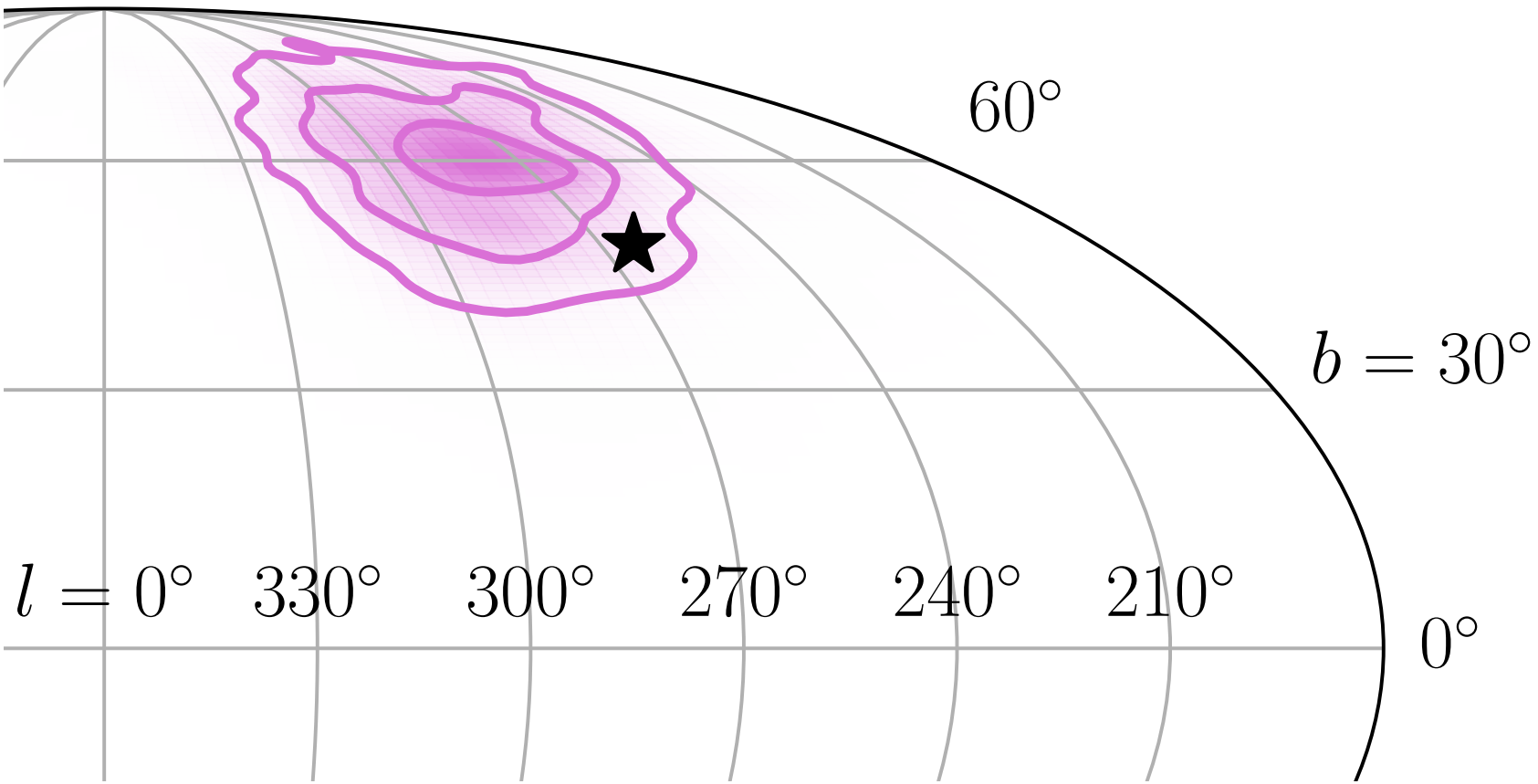

Figure 10: Projection of marginal distribution for l and b onto the sky, Galactic coordinates. ★: CMB dipole.

Clustering & Local Sources

Figure 11: ★*:* CMB dipole. *Red:* Results for NVSS. *Blue:* Results for RACS-low.

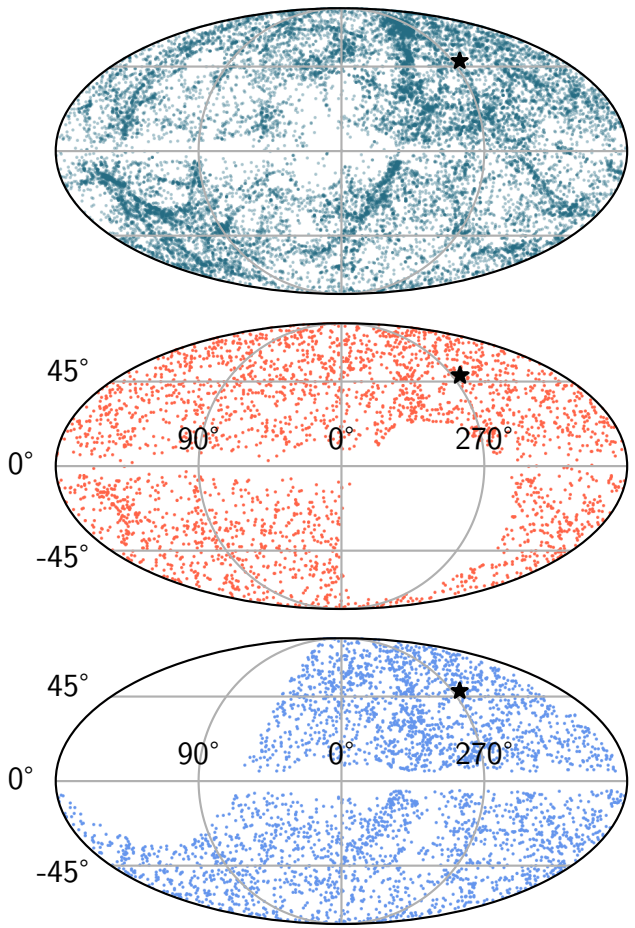

Clustering & Local Sources

Figure 11: ★*:* CMB dipole. *Red:* Results for NVSS. *Blue:* Results for RACS-low.

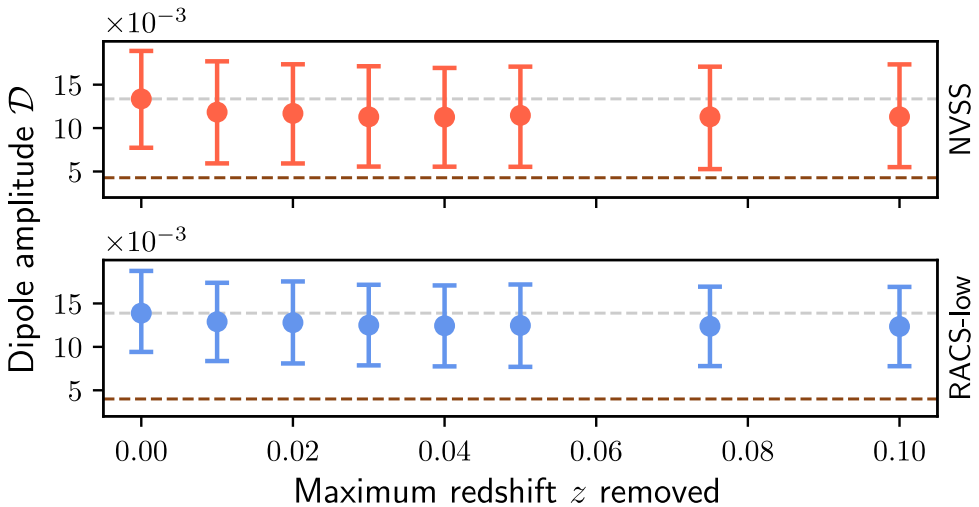

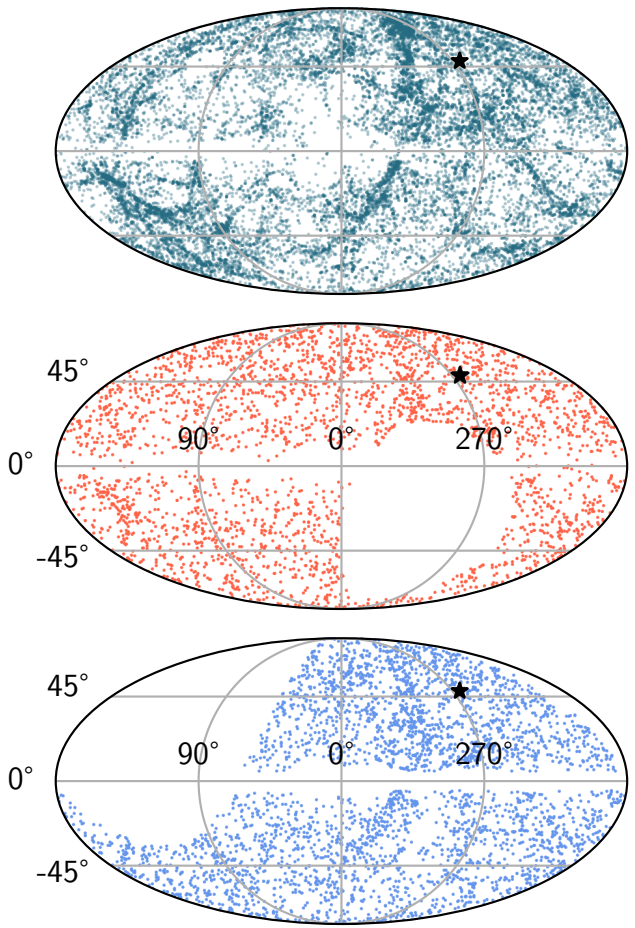

Clustering & Local Sources

Figure 11: ★: CMB dipole. *Red:* Results for NVSS. *Blue:* Results for RACS-low.

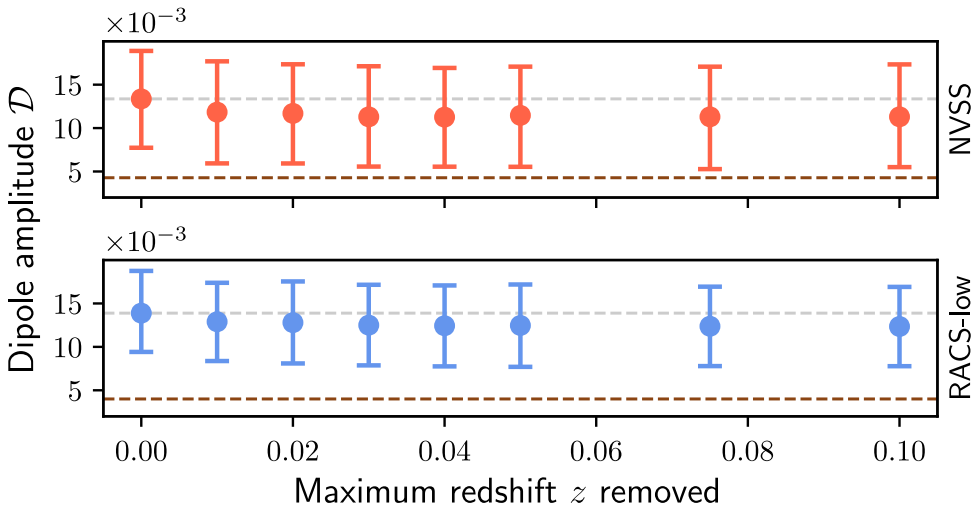

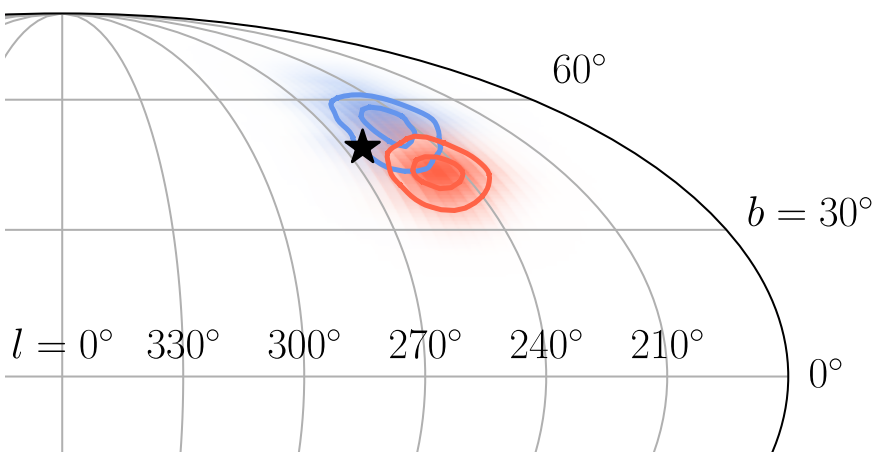

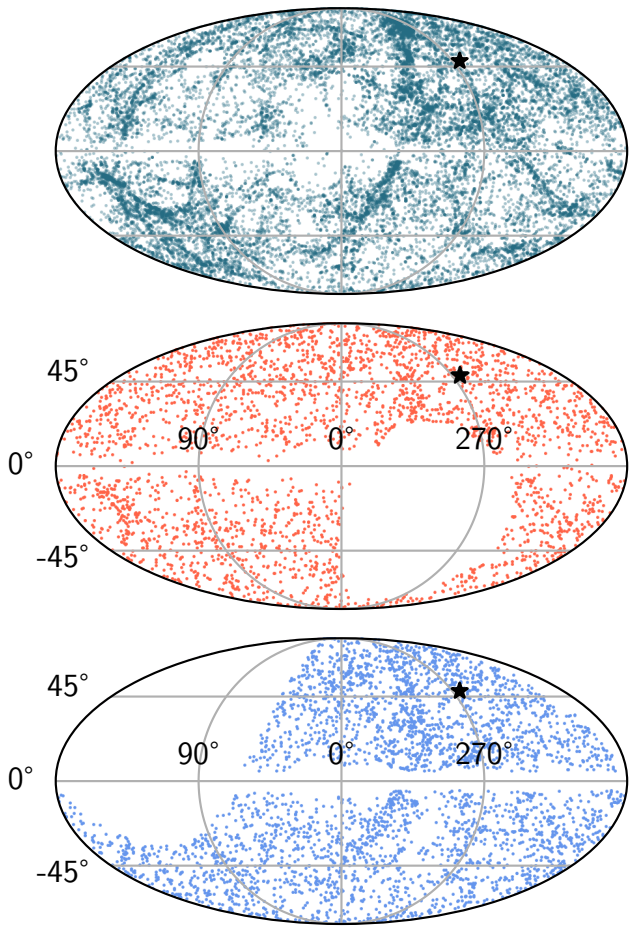

Discussion

Summary

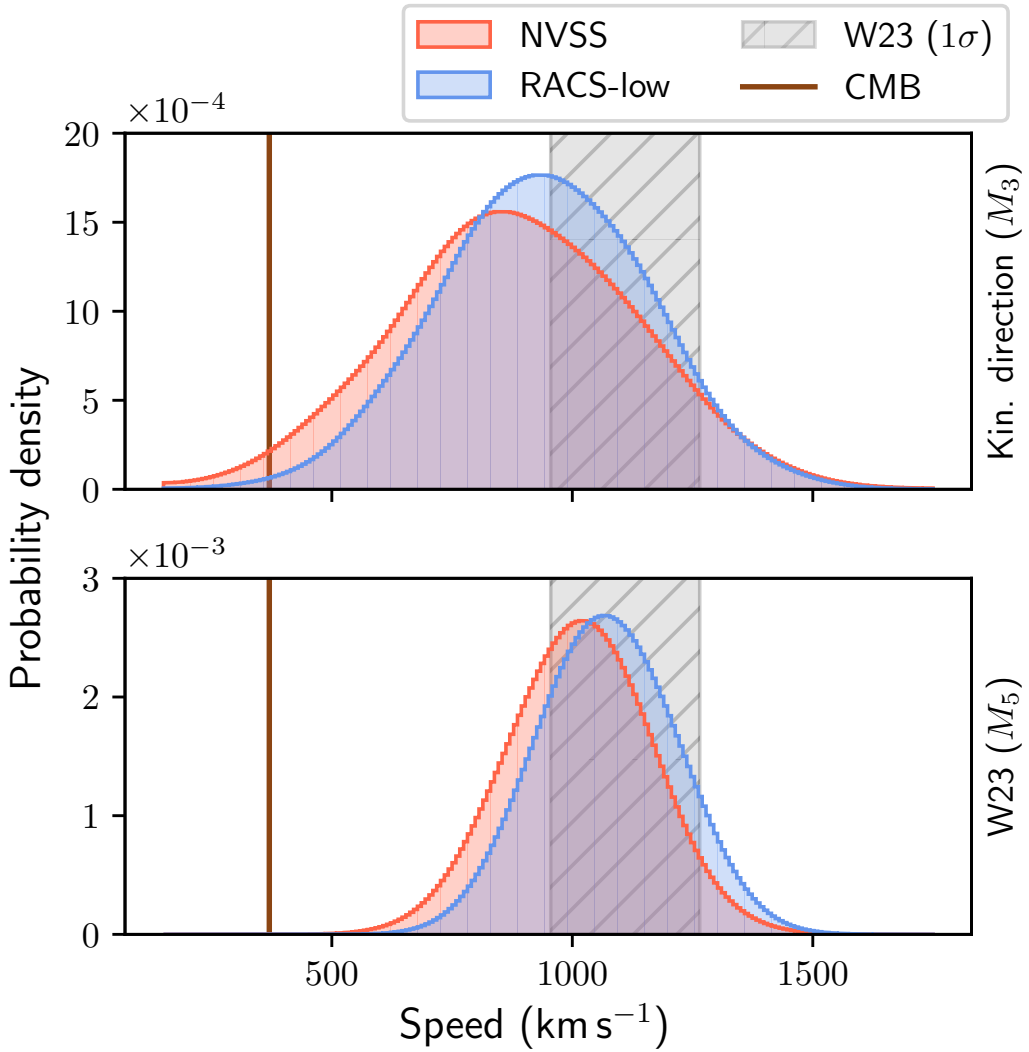
NVSS
RACS-low
W23 (1σ)
CMB
$\times 10^{-4}$
20
15
10
5
0
Kin. direction (M_3)
$\times 10^{-3}$
3
2
1
0
W23 (M_5)
Probability density
500
1000
1500
Speed (km s^{-1})

Summary

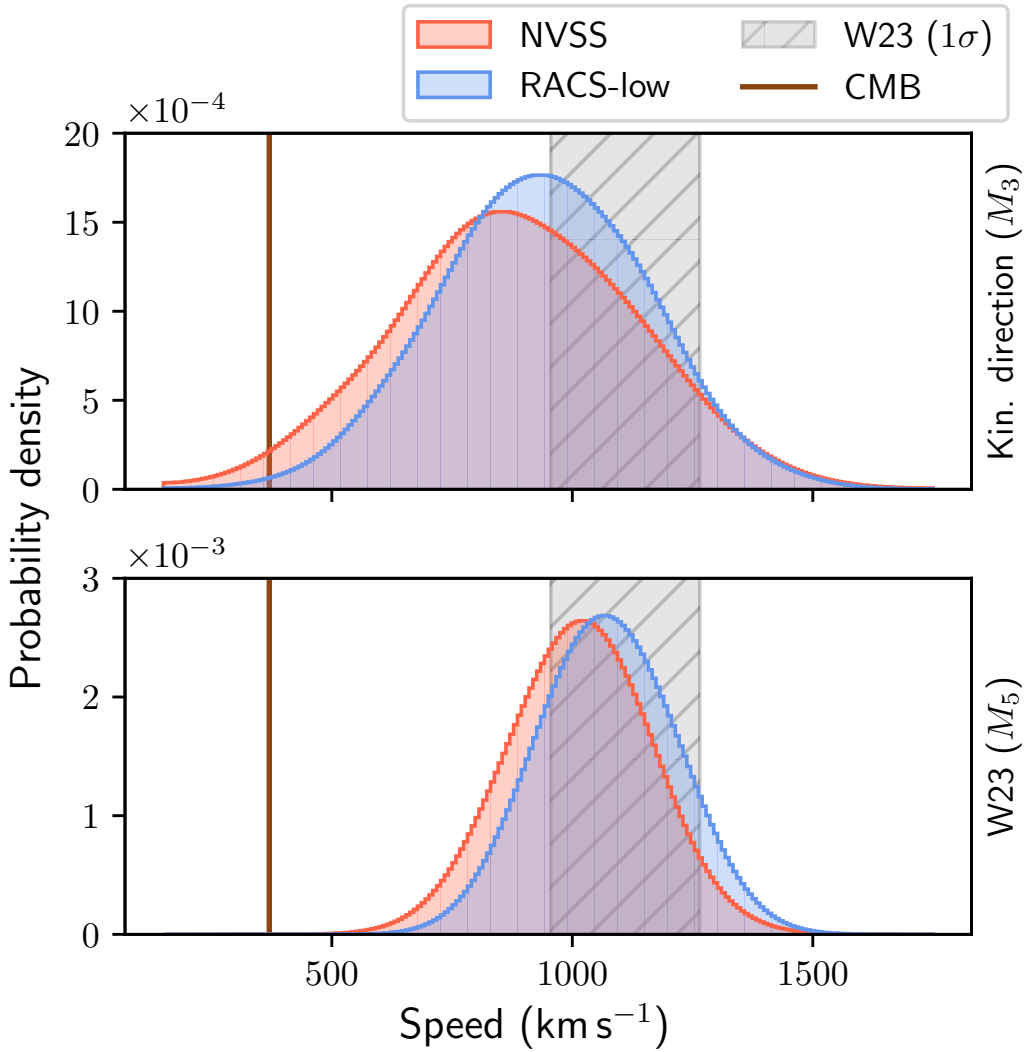

There is evidence for an excessive dipole in RACS/NVSS (2 to 3 $\times$ $\mathcal{D}_{\mathrm{CMB}}$).

Summary

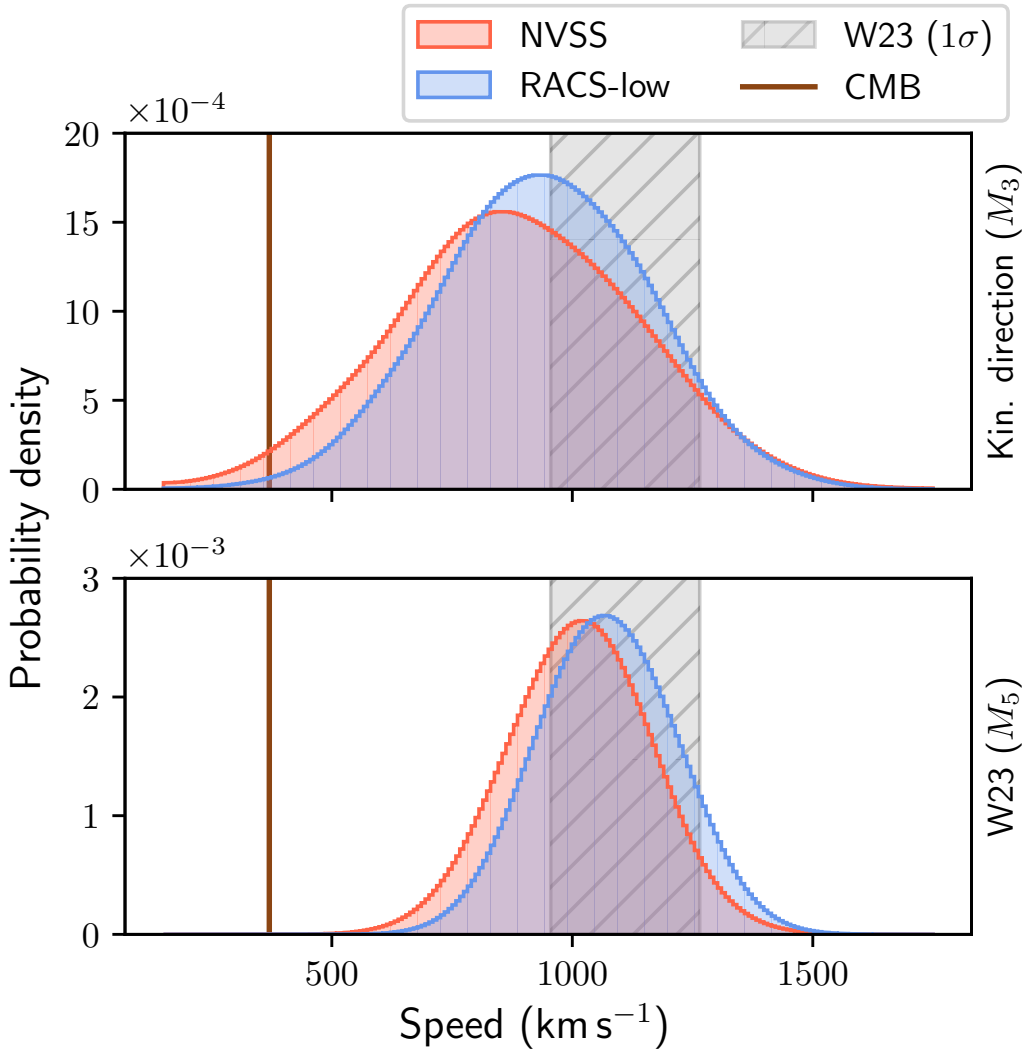

There is evidence for an excessive dipole in RACS/NVSS (2 to 3 $\times \mathcal{D}_{\mathrm{CMB}}$).

This corresponds to $v \approx 1000\,\mathrm{km\,s^{-1}}$, not $v_{\mathrm{CMB}} \approx 370\,\mathrm{km\,s^{-1}}$.

Summary

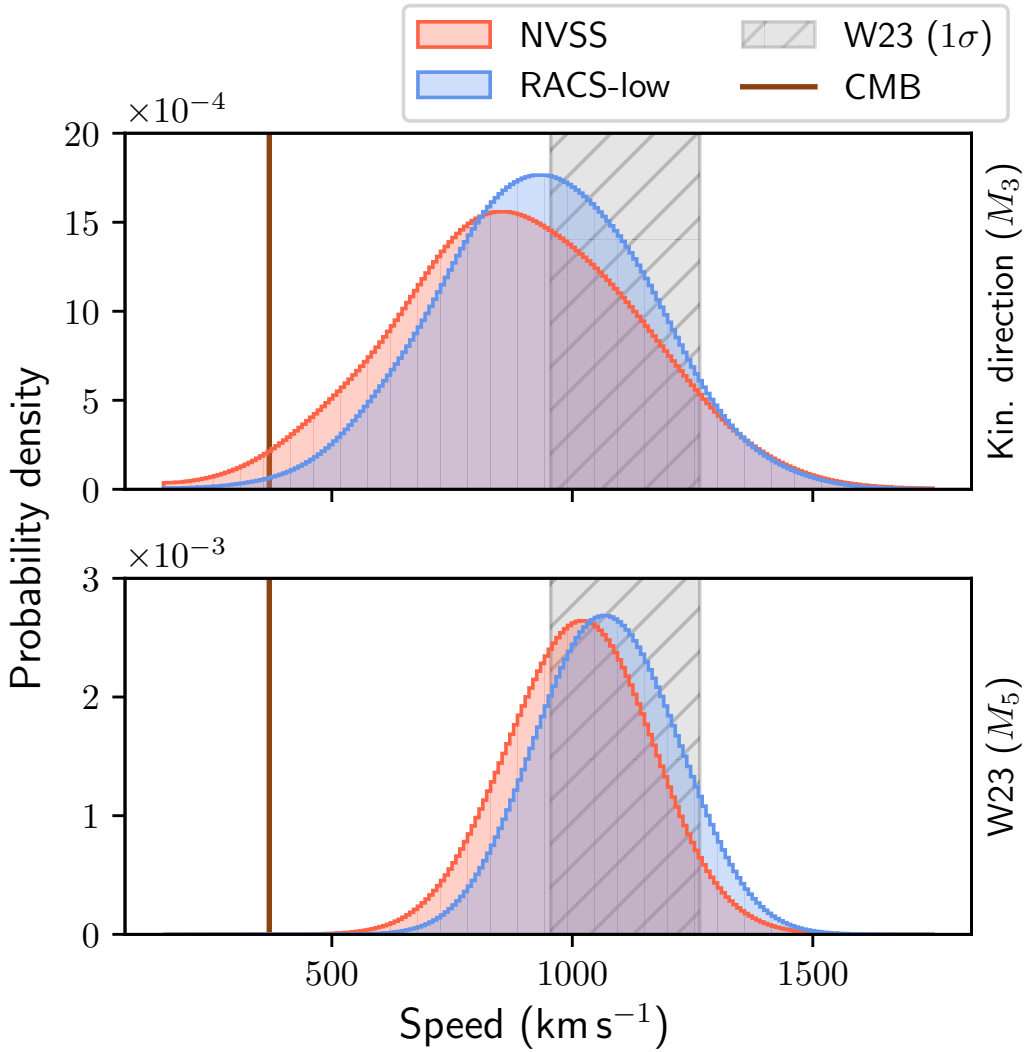

There is evidence for an excessive dipole in RACS/NVSS (2 to 3 $\times$ $\mathcal{D}_{\mathrm{CMB}}$).

This corresponds to $v \approx 1000\,\mathrm{km\,s^{-1}}$, not $v_{\mathrm{CMB}} \approx 370\,\mathrm{km\,s^{-1}}$.

The Hubble H_0 tension is $\approx 10\%$. This dipole tension is 100%–200% and has reached 5σ (see e.g. Secrest et al., 2021; Dam et al., 2023).

The Future — Investigating Systematics

The CatWISE2020 sample used in Secrest et al. (2021) has been questioned by Abghari et al. (2024).

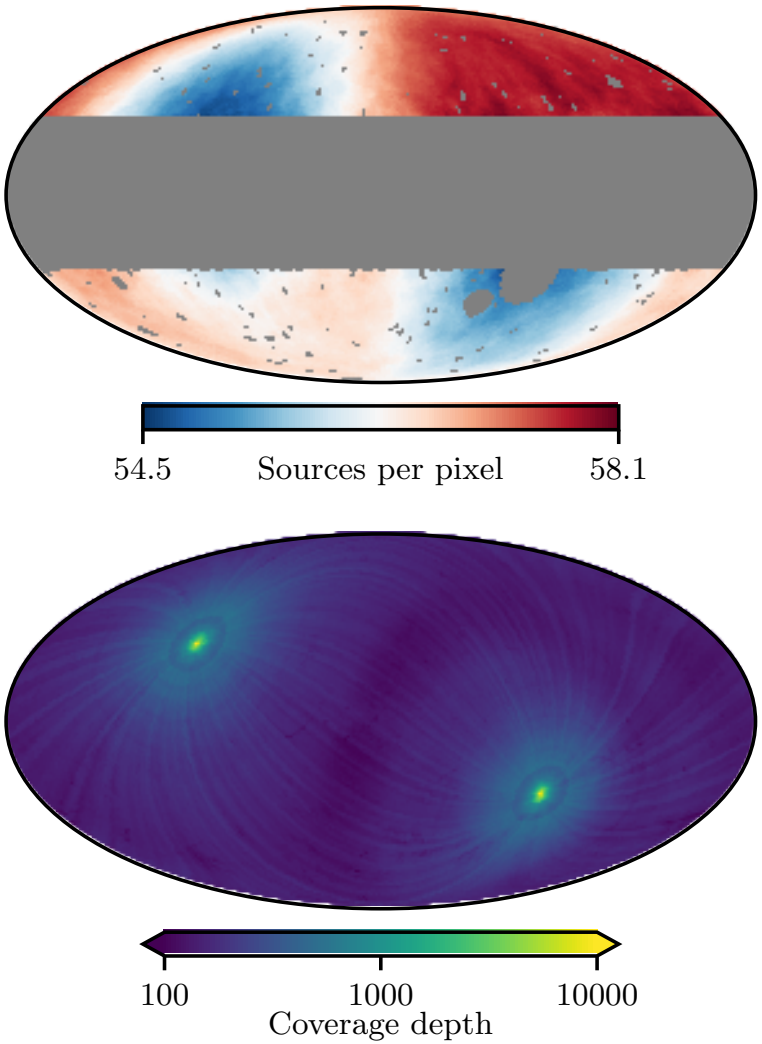

The Future — Investigating Systematics

The CatWISE2020 sample used in Secrest et al. (2021) has been questioned by Abghari et al. (2024).

What if there are additional, higher order multipoles on a masked sky? Mode coupling; power leakage.

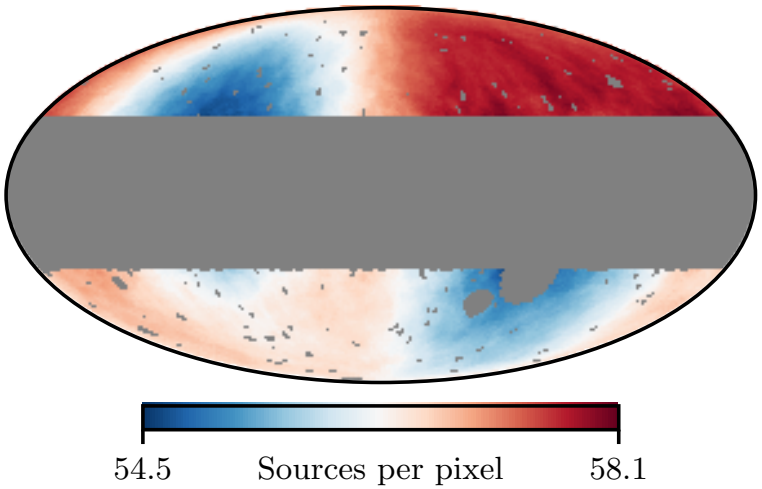

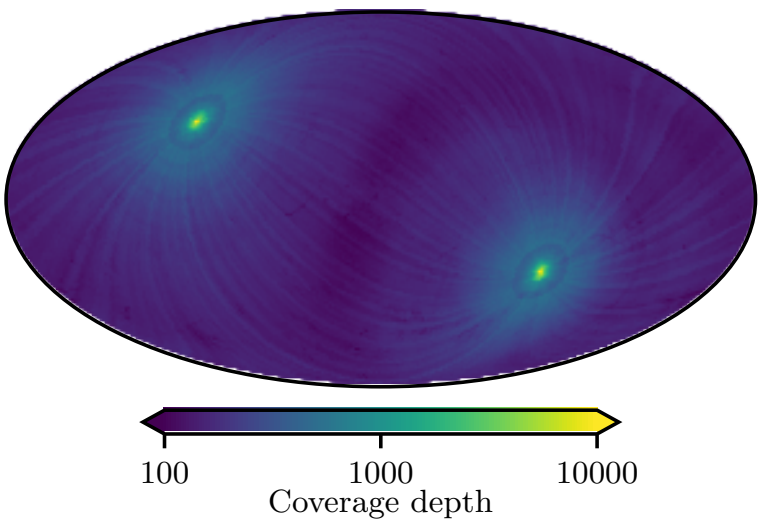

Figure 12: Plots from Abghari et al. (2024). *Right:* Smoothed CatWISE density map & scanning law. *Bottom:* Effect of additional multipoles on $\mathcal{D}$.

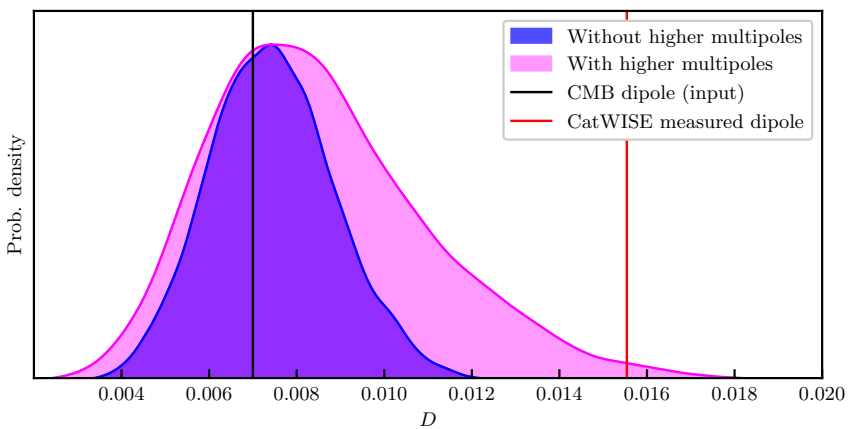

Dipole & Octupole

Figure 13: Results from fit to synthetic sample with intrinsic dipole ($\ell = 1$) and octupole ($\ell = 3$; Oayda et al., submitted).

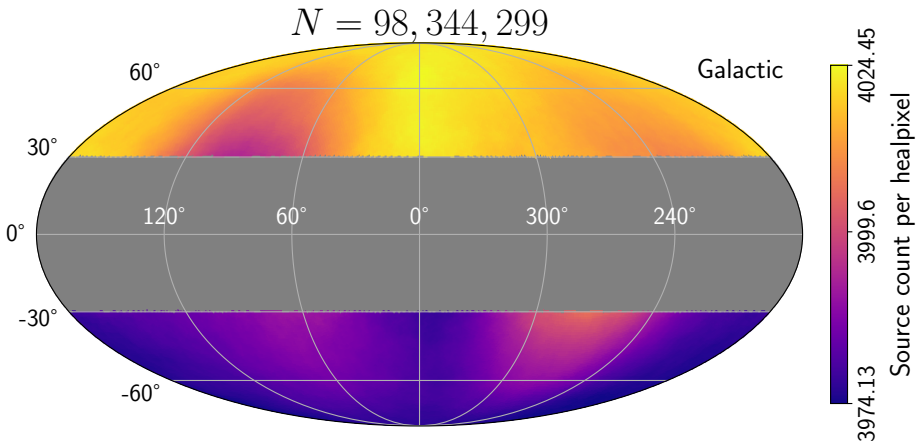

Dipole & Octupole

Figure 13: Results from fit to synthetic sample with intrinsic dipole ($\ell = 1$) and octupole ($\ell = 3$; Oayda et al., submitted).

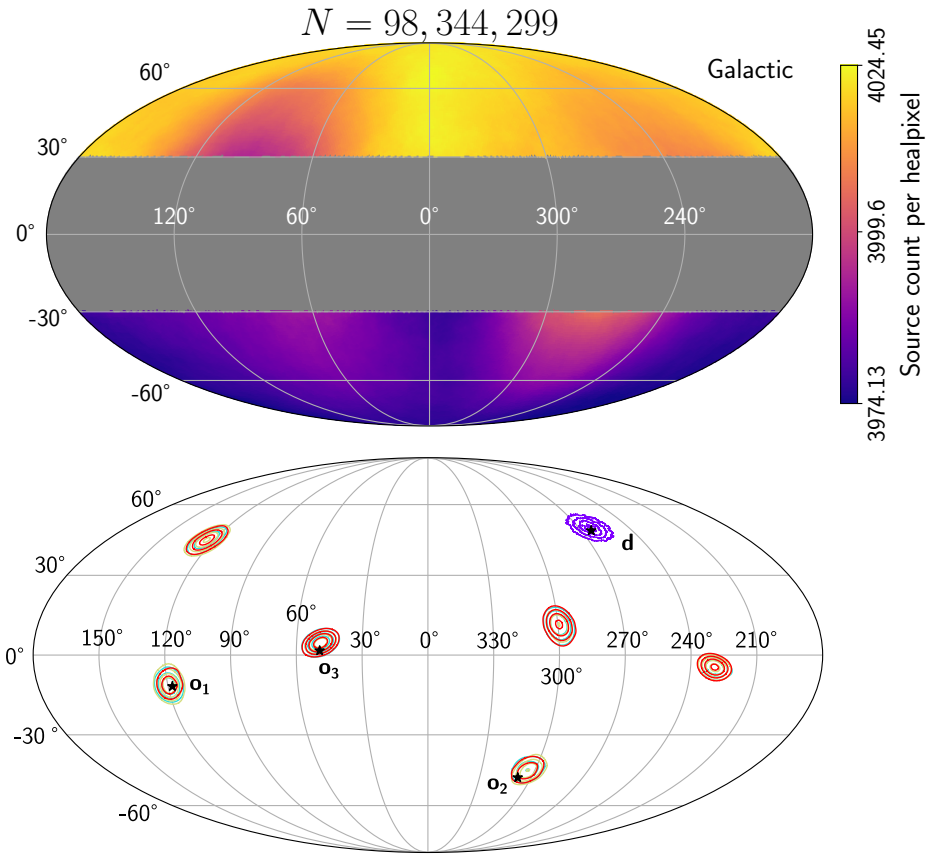

Dipole & Octupole

Figure 13: Results from fit to synthetic sample with intrinsic dipole ($\ell = 1$) and octupole ($\ell = 3$; Oayda et al., submitted).

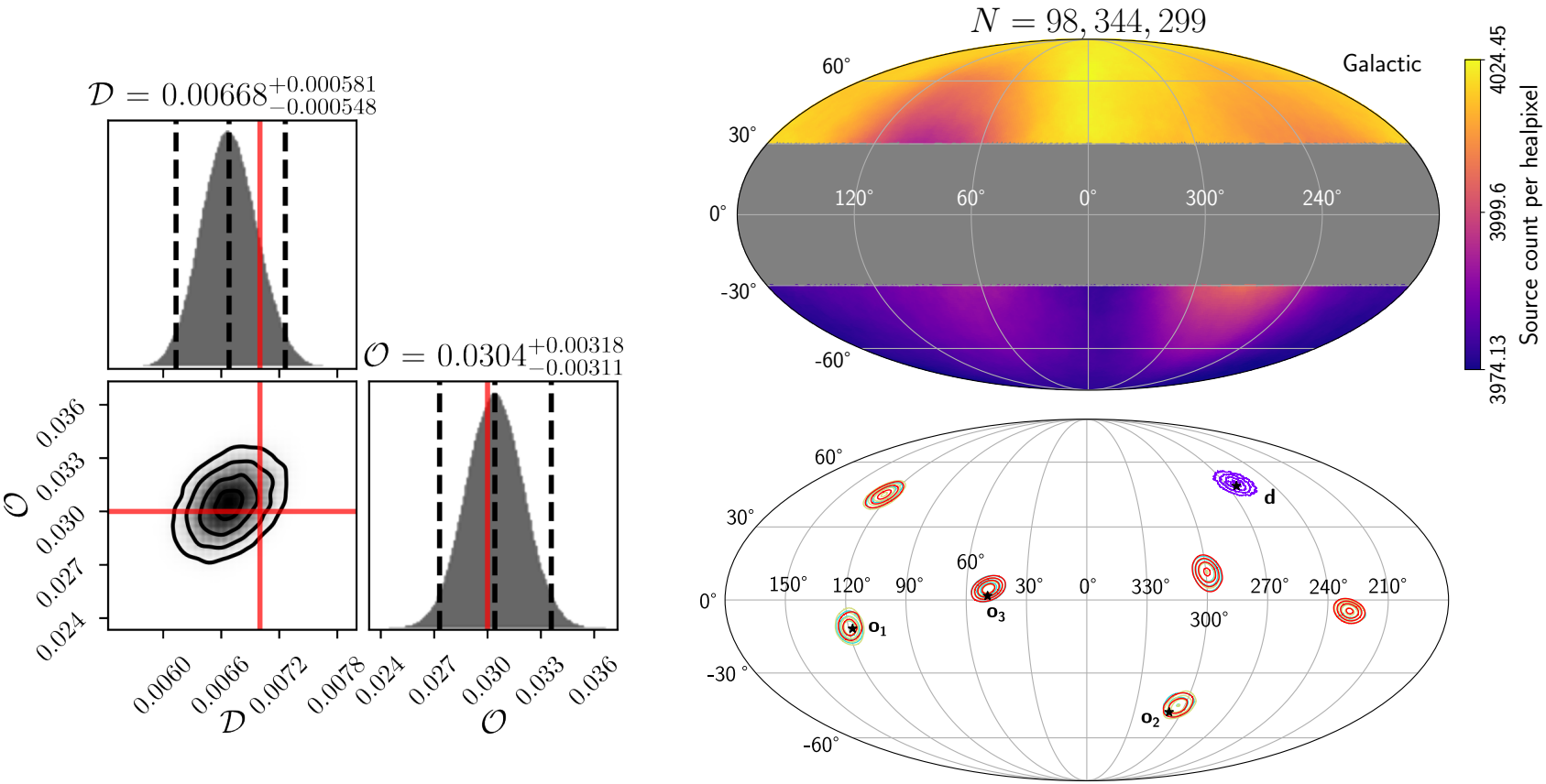

Dipole & Octupole

Figure 13: Results from fit to synthetic sample with intrinsic dipole ($\ell = 1$) and octupole ($\ell = 3$; Oayda et al., submitted).

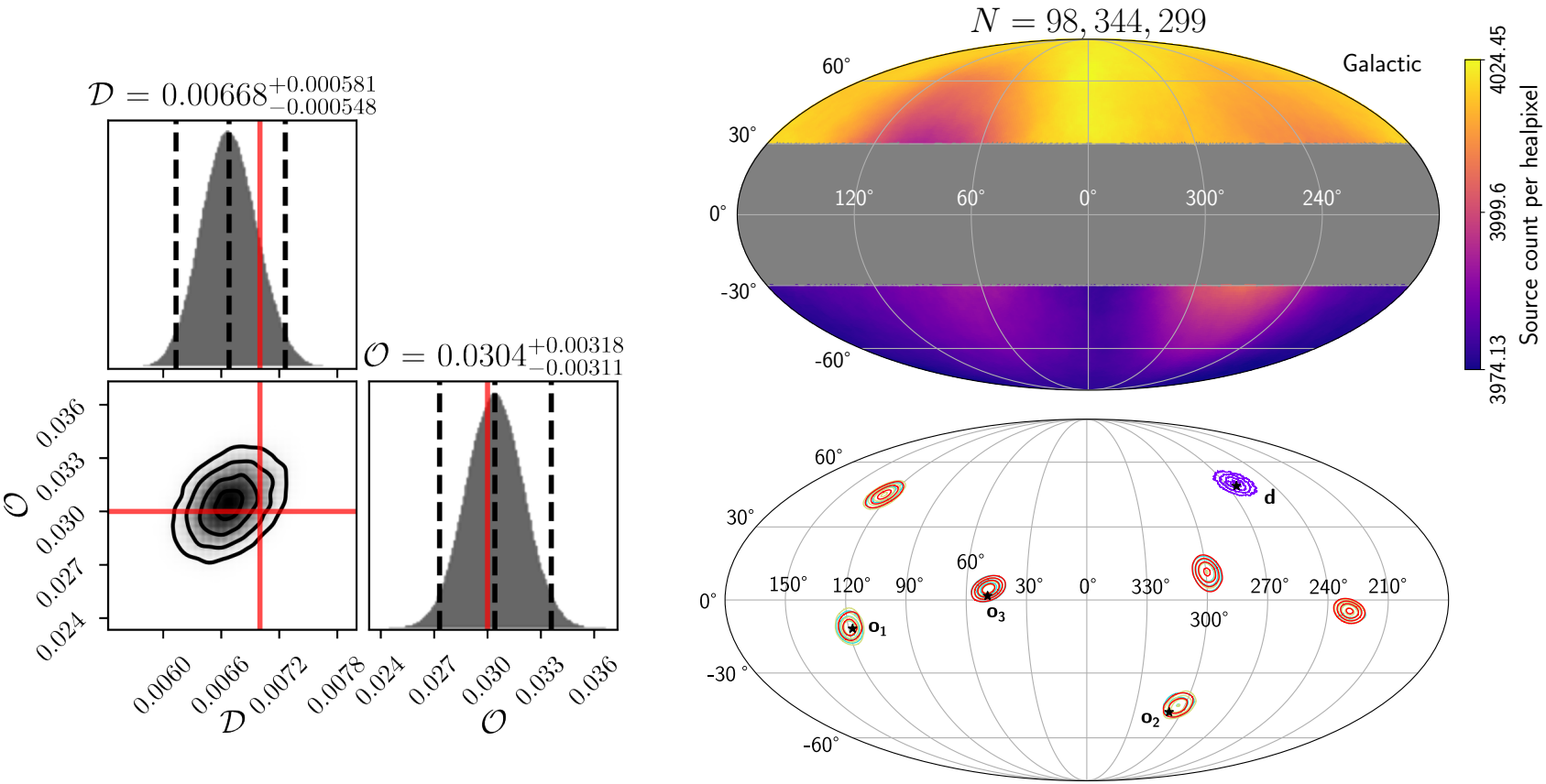

The dipole & octupole are disentangled from each other!

Why Multipoles?

We can use this approach as a diagnostic tool. For example...

Why Multipoles?

We can use this approach as a diagnostic tool. For example...

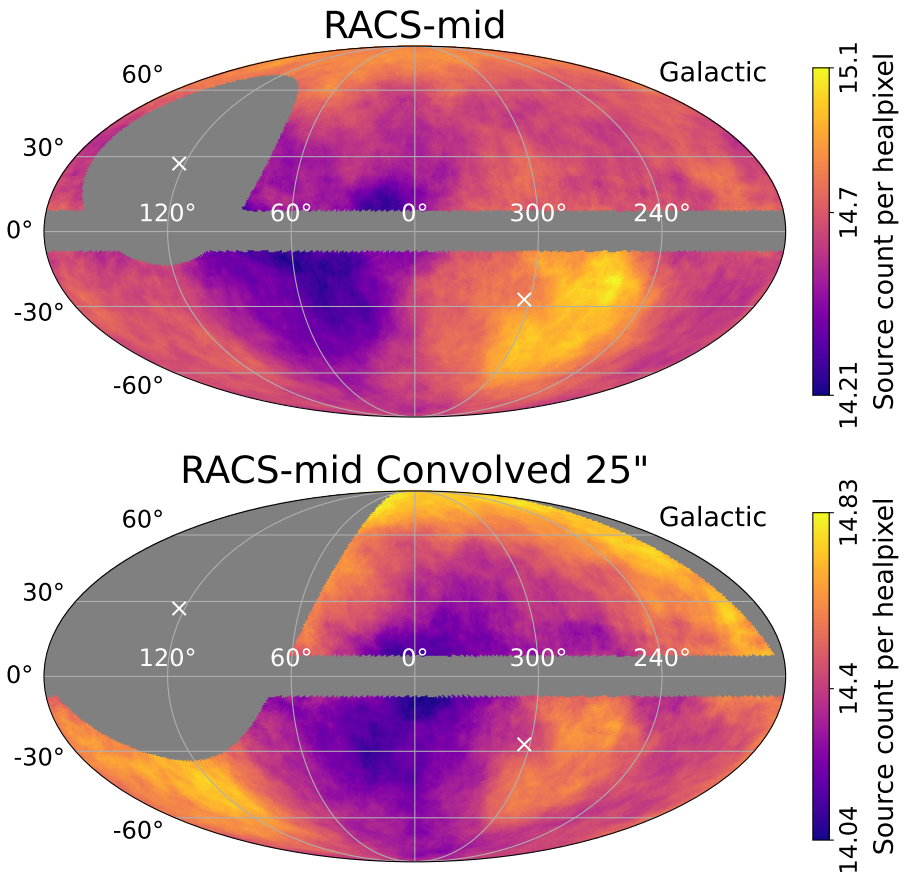

Figure 14: $10\,\mathrm{mJy} < S_{\mathrm{int.}} < 1000\,\mathrm{mJy}$. Smoothed RACS-mid maps (Galactic coordinates). *Top:* RACS-mid. *Bottom:* RACS-mid convolved to 25" common resolution.

Optimising Surveys

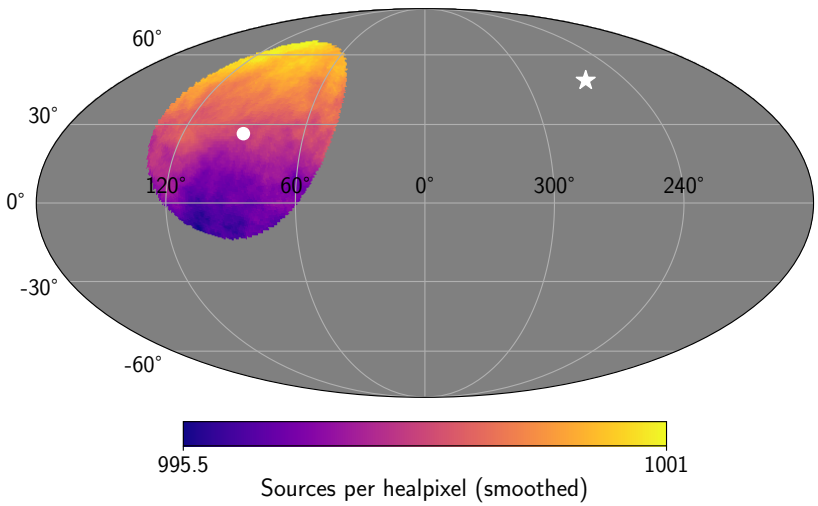

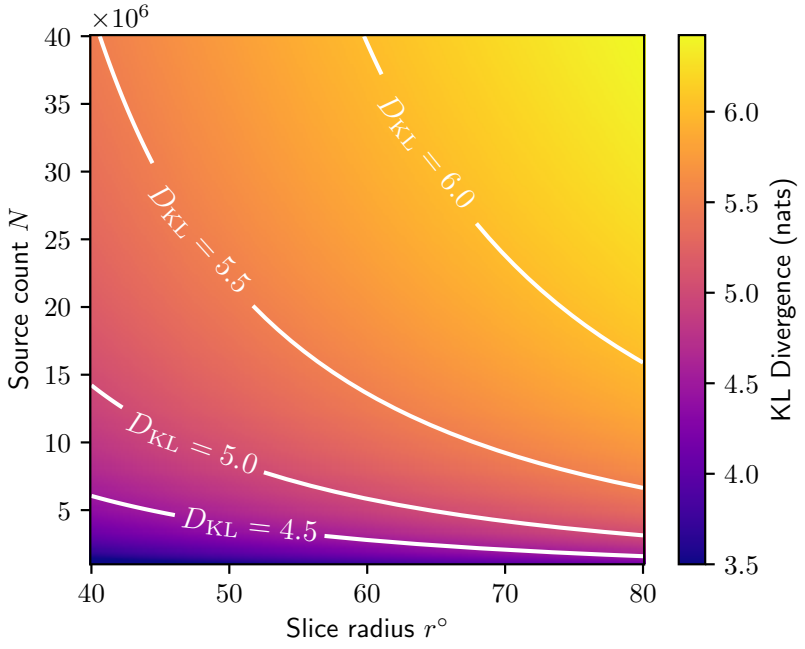

We're thinking about how out inferences change with surveys of different source counts and sky coverages.

EMU's anticipated $\approx$ 70 million sources (Norris et al., 2011) will be more than sufficient.

Conclusions

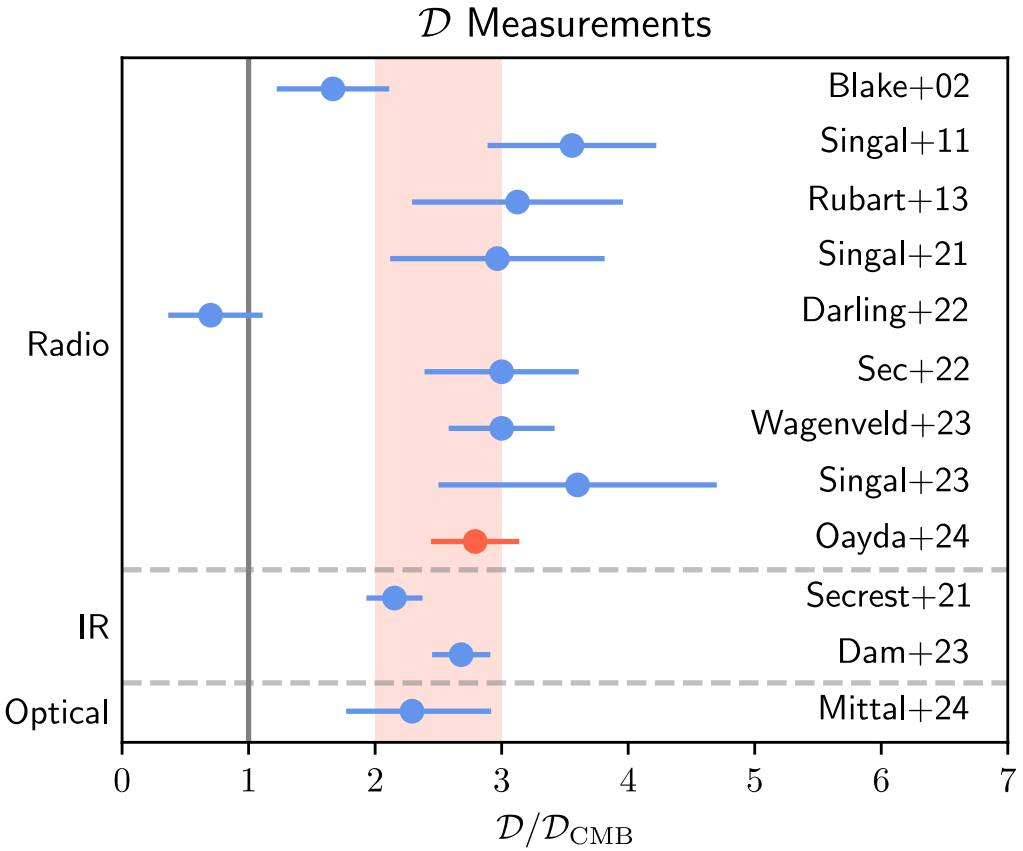

Figure 15: Literature values for $\mathcal{D}$ including results from our work (red) with RACS-low & NVSS and other studies (blue).

Key Finding

- RACS-low & NVSS dipole about a factor of 2 to 3 too large.
- We have to seriously investigate possible systematics.

References

Abghari A., Bunn E. F., Hergt L. T., Li B., Scott D., Sullivan R. M., Wei D., 2024, arXiv e-prints, p. arXiv:2405.09762

Dam L., Lewis G. F., Brewer B. J., 2023, MNRAS, 525, 231

Ellis G. F. R., Baldwin J. E., 1984, MNRAS, 206, 377

Mittal V., Oayda O. T., Lewis G. F., 2024, MNRAS, 527, 8497

Norris R. P., et al., 2011, PASA, 28, 215

Secrest N. J., von Hausegger S., Rameez M., Mohayaee R., Sarkar S., Colin J., 2021, ApJ, 908, L51

Secrest N. J., von Hausegger S., Rameez M., Mohayaee R., Sarkar S., 2022, ApJ, 937, L31

Springel V., et al., 2005, Nature, 435, 629

Wagenveld J. D., Klöckner H.-R., Schwarz D. J., 2023, A&A, 675, A72